

**JSCE- AIJ Joint Investigation/ Technical Support Team
for Restoration and Reconstruction
of the Affected Areas by the Pakistan Earthquake on
Oct. 8, 2005**

Nov. 2005



**Japan Society of Civil Engineers
Architectural Institute of Japan**

- Contents -

1 INTRODUCTION	2
2 GEOGRAPHY	8
3 GEOLOGY	10
4 TECTONICS	13
5 SEISMICITY	14
6 CRUSTAL DEFORMATION AND STRAINS	16
7 FAULTING CHARACTERISTICS AND SURFACE DEFORMATIONS	17
8 STRONG MOTIONS AND THEIR CHARACTERISTICS	25
9 DAMAGE TO CIVIL ENGINEERING STRUCTURES	31
9.1 Damage to Bridges	31
9.2 Damage to Roadways and Embankments	34
9.3 Damage to Tunnels	35
10 SLOPE FAILURES	37
10.1 Soil Slope Failures	38
10.2 Weathered Rock Slope Failures	40
10.3 Rock Slope Failures	43
11 RECOMMENDATIONS FOR REHABILITATION AND RESTORATION	46
11.1 Recommendations for Bridges	46
11.2 Recommendations for Roadway Embankments	50
11.3 Recommendations for Slope Cuts	50
11.4 Recommendations for Alternative Roadway Routes	52
11.5 Recommendations for Slope Stability Assessments	54
11.5.1 Macro-scale Stability Assessment	55
11.5.2 Site-specific Slope Stability Assessment	57
11.6 Recommendations for Slope Stabilization	65
11.7 Recommendations for Geotechnical Investigations for Damaged Civil Infra Structures & Slopes	67
11.7.1 Rapid Geotechnical Investigations	68
11.7.2 Detailed Geotechnical Investigations	69
11.8 Debris Management	72
12 CONCLUSIONS	73
REFERENCES	75

A QUICK REPORT ON 2005 KASHMIR EARTHQUAKE

JSCE

Investigation and Support Team
For Disaster Mitigation of
Oct. 8, 2005 Kashmir Earthquake

1 INTRODUCTION

A large devastating earthquake occurred in Kashmir on Oct. 8, 2005 at 8:50 (3:50UTC) local time of Pakistan. The depth of the earthquake was estimated to be about 10km and it had the magnitude of 7.6. The earthquake killed more than 75000 people, most of which was on Pakistani side of Kashmir. About 2000 people were killed in Indian side of Kashmir. The preliminary estimation indicated that the earthquake resulted from the subduction of Indian plate beneath Euroasian plate. The faulting mechanism solutions indicated that the earthquake was due to thrust faulting. Although there were no surface fracture as a result of the faulting, the valley between Muzaffarabad and Balakot may be the side where the fault should have appeared. The largest city influenced by the earthquake was Muzaffarabad, which is the capital of Pakistani Kashmir region. Balakot town was the nearest settlement to the epicenter and it was the most heavily damaged. Because of loose deposits resulting from steep slope degradation, it would have been extremely difficult to differentiate the effect of surface effects of the faulting. The earthquake caused extensive damage to housing and structures founded on these loose deposits. Furthermore, extensive slope failures occurred along Neelum valley, which obstructed both river flow and roadways.

JSCE dispatched its first investigation/ technical support team of four civil engineers to the severely damaged areas in Pakistan by the Pakistan Earthquake during the period from Oct. 24 to 30, 2005 in a close cooperation with the Ministry of Foreign Affairs of Japan and Japan International Cooperation Agency (JICA). The JSCE team studied and assessed the damages caused to bridges, buildings, embankments and slopes, and also exchanged opinions about the results of the assessment of the damages to structures and facilities as well as the methods of temporary repairs, restorations and reconstructions with authorities and engineers from the related Pakistani organizations such as Capital Development Authority (CDA) and National Highway Authority (NHA).

In the exchanges, the members from the Japanese team were strongly requested from

the Pakistani engineers to share the technologies and knowledge, which have been accumulated through the experiences of many earthquake-related-disasters in Japan on the following themes:

1. **Methods of the temporary repairs and reconstructions of damaged road facilities including bridges and embankments based on more detailed assessment**
2. **Assessment of damaged buildings and the methods of temporary repairs and reconstructions**
3. **Assessment of slope stability, temporary measures and permanent protection measures**

In order to respond to the above-mentioned requests, JSCE and AIJ had organized and decided to dispatch the investigation/ technical support team to Pakistan from the 18th to 28th of November (See list of members and itinerary of the team). After the completion of damage investigation in the affected areas (Figure 1.1), the team held seminars at NHA and CDA separately on the three issues mentioned above as well as the results of its investigation for the relevant authorities and engineers. This report describes an overall view of geology, tectonics, seismicity and structural as well as geotechnical damages concerning civil engineering structures and buildings. The final part of this report the recommendations of the team for the temporary and permanent restoration and re-construction of the earthquake affected civil engineering structures.

TEAM MEMBERS

Dr. Masanori HAMADA (Leader)		
Position	Professor, Waseda University	
Specialty	Earthquake Engineering	
Phone	+81-3-3208-0349	
Fax	+81-3-3208-0349	
e-mail	Hamada@waseda.jp	
URL	http://www.waseda.jp/sem-hamada01/	
Dr. Kazuo KONAGAI		
Position	Professor, Institute of Industrial Science, The University of Tokyo	
Specialty	Geotechnical Earthquake Engineering	
Phone	+81-3-5452-6142	
Fax	+81-3-5452-6144	
e-mail	konagai@iis.u-tokyo.ac.jp	
URL	http://shake.iis.u-tokyo.ac.jp/home/	
Dr. Ömer AYDAN		
Position	Professor, Tokai University	
Specialty	Rock Mechanics and Earthquake Engineering	
Phone	+81-543-34-0411	
Fax	+81-543-34-9768	
e-mail	Aydan@scc.u-tokai.ac.jp	
URL	http://www.scc.u-tokai.ac.jp/ocean/oc/labs/aydan.htm	

Dr. Masakatsu MIYAJIMA		
Position	Professor, Kanazawa University	
Specialty	Geotechnical Earthquake Engineering	
Phone	+81-76-234-4656	
Fax	+81-76-234-4656	
e-mail	miyajima@t.kanazawa-u.ac.jp	
URL	http://www.ad.kanazawa-u.ac.jp/souran/kekka/shosai.asp?id=749	
Mr. Takeshi KOBAYASHI		
Position	Executive Director, Expressway Technology Center	
Specialty	Highway, Bridge, Traffic, Landscape	
Phone	+81-3-3503-2314	
Fax	+81-3-3503-2308	
e-mail	t_kobayashi@extec.or.jp	
URL	http://www.extec.or.jp	
Dr. Takao NISHIKAWA		
Position	Professor, Tokyo Metropolitan University	
Specialty	Geotechnical Earthquake Engineering	
Phone	+81-426-77-2803	
Fax	+81-426-77-2793	
e-mail	tanishi@arch.metro-u.ac.jp	
URL	-	
Dr. Yoshiaki NAKANO		
Position	Professor, Institute of Industrial Science, The University of Tokyo	
Specialty	Earthquake Engineering of Building Structures	
Phone	+81-3-5452-6145	
Fax	+81-3-5452-6146	
e-mail	iisnak@iis.u-tokyo.ac.jp	
URL	http://sismo.iis.u-tokyo.ac.jp/index-e.html	
Dr. Yasushi SANADA		
Position	Research Associate, ERI, The University of Tokyo	
Specialty	Reinforced Concrete and Masonry Buildings	
Phone	+81-3-5841-5783	
Fax	+81-3-5689-7265	
e-mail	ysanada@eri.u-tokyo.ac.jp	
URL	http://www.eri.u-tokyo.ac.jp/saigai/index.html	
Mr. Noboru KONDO		
Position	Adviser, NHA/JICA	
Specialty	Highway, Bridge, Traffic	
Phone	+92-51-926-1386	
Fax	+92-51-926-1386	
e-mail	noboru@comsats.net.pk	
URL		

Mr. Shigeki TAKATSU		
Position	Researcher, Japan Society of Civil Engineers	
Specialty	Geology	
Phone	+81-3-5452-6612	
Fax	+81-3-5452-6613	
e-mail	takatsu@iis.u-tokyo.ac.jp	
URL	-	
Mr. Hiromi SAMESHIMA		
Position	General Manager of Pakistan Office, Tobishima Corporation	
Specialty	Building Engineer	
Phone	+92-300-852-5112	
Fax	+92-51-2650285	
e-mail	sametobi@comsats.net.pk	
URL	http://www.tobishima.co.jp	
Mr. Hiroyuki KODAMA		
Position	Manager, Tobishima Corporation	
Specialty	Civil Engineering	
Phone	+81-3-5214-7081	
Fax	+81-3-5276-2526	
e-mail	hiroyuki_kodama@tobishima.co.jp	
URL	http://www.tobishima.co.jp	
Mr. Yoshihiro TSUCHIYA		
Position	Chief Engineer, Tobishima Corporation	
Specialty	Earthquake-Resistant and of Building	
Phone	+81-3-5214-7098	
Fax	+81-3-3221-6458	
e-mail	yoshihiro_tsuchiya@tobishima.co.jp	
URL	http://www.tobishima.co.jp	

Itinerary: Nov. 18 ~ 28, 2005

Date	Itinerary	Stay at
Nov. 18 (Fri.)	1) Leave for Pakistan (Dr. Nakano, Dr. Sanada, Mr. Kodama and Mr. Tsuchiya) PK853: Departure from Narita at 14:00/ Arrival at Islamabad at 21:05	Islamabad
19 (Sat.)	1) 10:00 Preliminary survey of Margalla Tower, AL.Mustafa Tower, Park Tower (Guide: CDA) 2) Inspection of Alsafa Heights, Sula Tower (buildings under construction in Islamabad)	Islamabad
20 (Sun.)	1) Preliminary survey of school in Battal	Islamabad
21 (Mon.)	1) Preliminary survey in Muzaffarabad ----- Leave for Pakistan (Dr. Hamada, Dr. Konagai, Dr. Aydan, Mr. Kobayashi, Dr. Nishikawa, Dr. Miyajima and Mr. Takatsu) PK853: Departure from Narita at 14:00/ Arrival at Islamabad at 21:05	Islamabad
22 (Tue.)	1) Team meeting 2) Courtesy visits to: 09:00 Geological Survey of Pakistan 11:30 National Highway Authority (NHA) 12:30 Capital development Authority (CDA) 14:30 JICA / JBIC 16:00 the Embassy of Japan in Pakistan	Islamabad
23 (Wed)	1) Leave for Balakot: Departure from Islamabad at 6:00/ Arrival at Balakot at 10:00 2) Survey in Balakot 3) Leave for Nathiagali: Departure from Balakot at 15:30/ Arrival at Nathiagali at 18:00 ----- Return to Japan (Dr. Konagai) TG510: Departure from Islamabad at 24:05 (00:05, Nov. 24)/ Arrival at Bangkok at 06:45 TG676: Departure from Bangkok at 8:20/ Arrival at Narita at 16:00, Nov. 24	Nathiagali
24 (Thu.)	1) Leave for Muzaffarabad/ Departure from Nathiagali at 7:00/ Arrival at Muzaffarabad at 10:00 2) Survey Jhelum Valley Road and Bridges 3) Survey in Muzaffarabad 4) Return to Islamabad: Departure from Muzaffarabad at 14:30/ Arrival at Islamabad at 18:00 ----- Return to Japan (Dr. Miyajima) PK852: Departure from Islamabad at 22:50/ Arrival at Narita at 12:50, Nov. 25	Islamabad
25 (Fri.)	1) 09:00 Inspection of Margalla Tower (Guide: CDA) 2) 10:00 visit to Ministry of Communication (Dr. Hamada & Dr. Nishikawa) 3) 11:00 visit to Earth Quake Reconstruction & Rehabilitation Authority 4) Team meeting, Preparations for seminars	Islamabad
26 (Sat.)	1) Seminars at: 09:30-12:00 NHA: Venue: Auditorium in NHA 15:00-17:00 CDA & Institute of Architect of Pakistan: (Venue: Convention Centre) 2) Press conference ----- 3) Return to Japan (Dr. Hamada, Dr. Aydan, Dr. Nishikawa, Dr. Nakano and Dr. Sanada) TG510: Departure from Islamabad at 24:05 (00:05, Nov. 27)/ Arrival at Bangkok at 06:45 JAL708: Departure from Bangkok at 8:20/ Arrival at Narita at 16:05, Nov. 27	Islamabad

27 (Sun.)	1) Team Meeting 2) Return to Japan (Mr. Kobayashi, Mr. Takatsu and Mr. Tsuchiya) PK852: Departure from Islamabad at 22:50/ Arrival at Narita at 12:50, Nov. 28	
28 (Mon.)	1) Arrival at Narita	

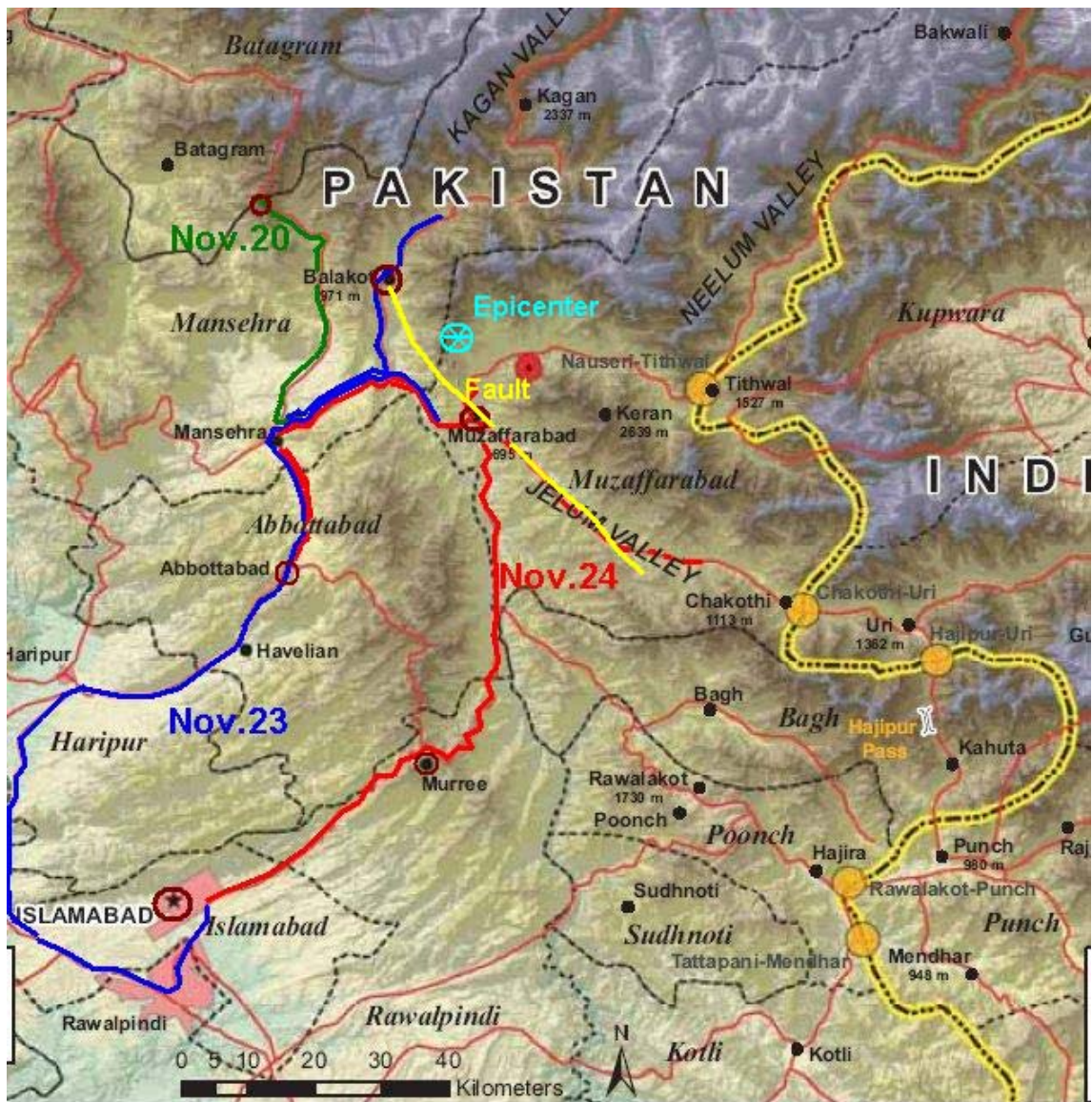


Figure 1.1 Investigations routes of the team of JSCE and AIJ

2 GEOGRAPHY

The earthquake occurred in Kashmir Region. The largest city nearby the epicenter is Muzaffarabad (10.7km NE) with a population of 660000. The other nearest cities are Manshera and Abbotabad (Figures 2.1,2.2 and 2.3). The area is very mountainous and it consists of very deep valleys. Several branches of Indus rivers such as Neelum and Jhelum pass through the area. The Jhelum river, which has its source in the Varing spring in the Anantnag (Islamabad) district of Kashmir, enters near Chakoti at the confluence of Urusa Nala and flows in a southeast to north-west directions up to Muzaffarabad where Neelum river joins it. Then after it runs toward south along the border of Azad Kashmir and Pakistan. The Neelum River, which was formerly known as Kishan Ganga has also its source in the Indian side of Kashmir and enter the district in Athmuqam tehsil and flows through Neelum valley.



Figure 2.1: Kashmir region

Neelum Valley is about 200 Km long and it is situated at the North & North-East of Muzaffarabad, running parallel to Kaghan Valley. The two valleys are only separated by snow-covered peaks which are over 4000m above sea-level. Jhelum River passes through from East to West between the high mountains joining river Neelum at Domel in Muzaffarabad. An artificial lake at Subri created due to a slope failure of the surrounding mountain during 1975.

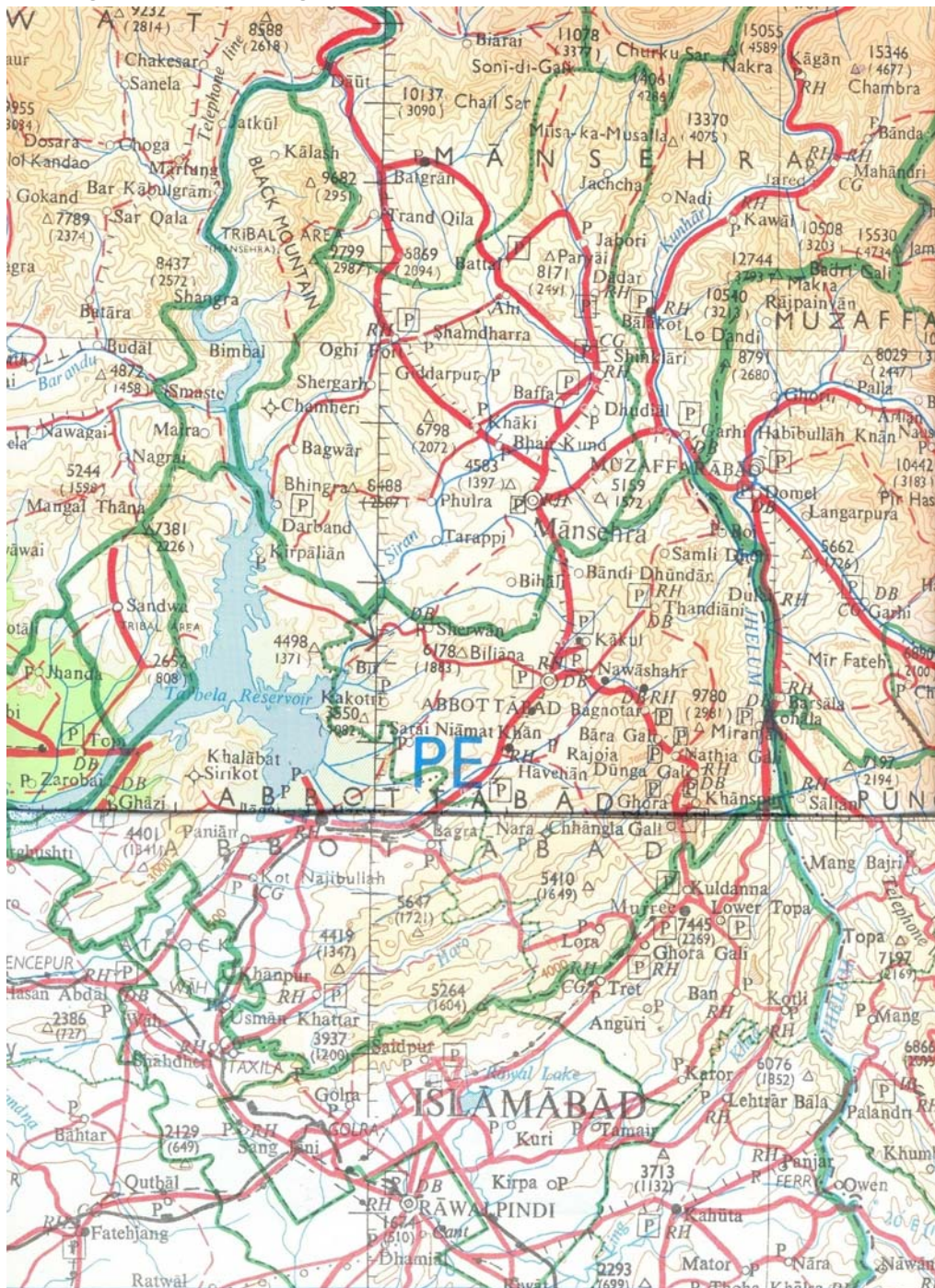


Figure 2.2: Close-up map of epicentral area

3 GEOLOGY

In northern Pakistan the orogen is composed of three main tectonostratigraphic terranes (Figure 3.1): the Asian plate to the north, the Indian plate to the south, and the Kohistan island arc sandwiched between. The Kohistan arc is separated from the Asian plate by the Northern or Shyok Suture and from the Indian plate by the Main Mantle Thrust (MMT). The Asian plate Karakoram can be divided into the Northern Sedimentary terrane of Palaeozoic and Mesozoic Formations, the Karakoram Batholith of Cretaceous to Miocene age, and the Kohistan arc consists of Late Cretaceous and Eocene plutonic belts, and pyroxene granulites, calc-alkaline volcanics, amphibolites, and minor metasediments. The Indian plate can be subdivided into three tectonic units: From north to south these are (1) an internal metamorphosed unit, (2) an external unmetamorphosed or low-grade metamorphic unit, and (3) the foreland basin sediments. The internal unit consists of cover and basement rocks. The basement rocks are predominantly high-grade gneisses, the cover rocks are predominantly greenschist to amphibolite grade metapelites and metapsammites metamorphosed during the Himalayan orogeny. The internal zone is separated from the external zone unmetamorphosed to low-grade metamorphic Precambrian sediments and dominantly Mesozoic to Eocene Tethyan shelf sediments by the Panjal Thrust (PT). Farther to the south, the Main Boundary Thrust (MBT) separates these rocks from the Tertiary foreland basin deposits. The Main Frontal Thrust (MFT) delineates the southernmost extent of the foreland basin fold and thrust belt.

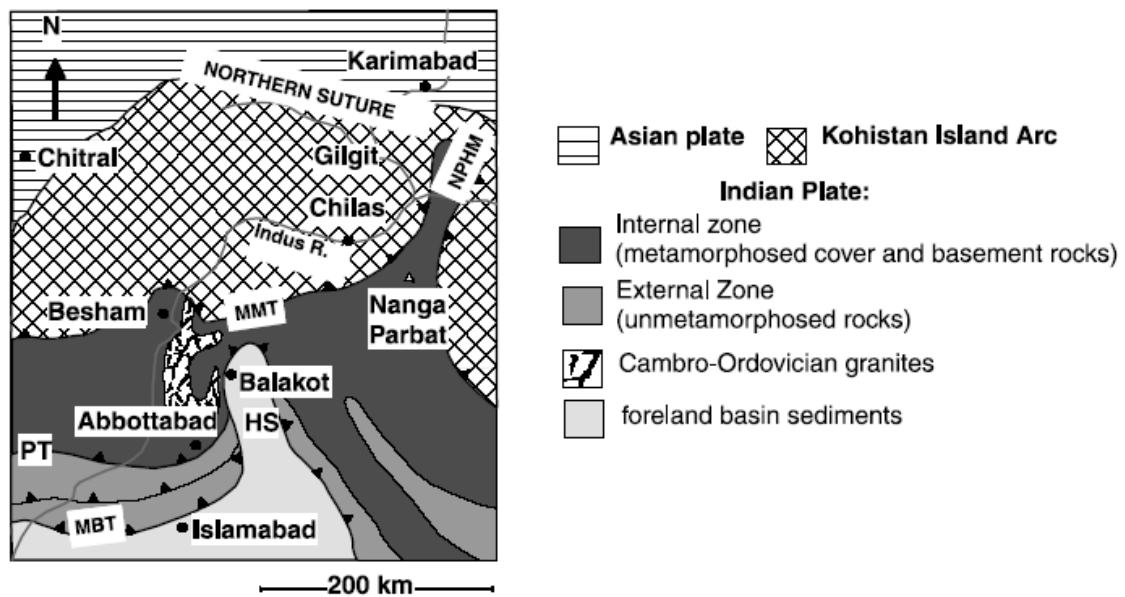


Figure 3.1: Regional Geology of Kashmir

The >8 km thick red bed Balakot Formation in the Hazara-Kashmir Syntaxis as a steeply north dipping, normal homoclinal stratigraphic succession, conformably overlying the Paleocene-aged shallow marine Patala Formation and Lockhart Limestone. The Balakot Formation is actually variably deformed and folded by a series of tight folds (wavelength and amplitude of 1 km) (Figures 7b and 8). From Balakot to Paras, the beds of the Balakot Formation follow a series of anticlines and synclines that intensify in tightness toward the middle of the section. The surface distribution of the marl bands coincides with high-strain zones localized in the hinge zones of folds. The marl bands coincide in the field with chlorite grade high-strain zones. These zones are characterized by highly discontinuous and transposed bedding. The structural style of the Balakot Formation, in which the marl units are part of an underlying formation, exposed by subsequent deformation related to shear folding and associated faulting. The Balakot Formation conformably overlies the Paleocene deposits consisting mainly of the Lockhart limestone and the shales and marls of the Patala Formation. The Patala and Lockhart Formations to unconformably overlie the Late Precambrian to Cambrian Abbotabad Formation, which forms the core of the Muzaffarabad anticline. The lower part the Balakot Formation is structurally imbricated and isoclinally folded with the Patala Formation, which in turn is in thrust contact with the overlying Abbotabad limestones. The entire package is complexly faulted, with systematic top to the southwest thrust shear sense. Therefore, in summary, the Balakot Formation red beds lie in thrust contact with the Paleocene aged shallow marine Patala Formation and Lockhart Limestone below, and are tectonically intercalated with an underlying dark gray marl formation.

The Balakot Formation red bed succession shows fining up sequences, often beginning with thick-bedded, medium-grained sandstones which are quite commonly erosively based and/or channel lagged, with rare groove and flute marks and cross beds. Overlying these sandstones, thinner-bedded and finer-grained sandstones are often found, sometimes separated by thin undulating muddraped beds. Thick mudstones at the top of the cycle can be interbedded with thin or medium-bedded siltstones and sandstones. Caliche is also present. Sedimentary structures present in the sandstones include grading, asymmetrical ripple marks, flasers, climbing ripples, convolute bedding, load and flame and parallel laminations. Interlaminations of mudstone and sandstone on a fine scale are also present.

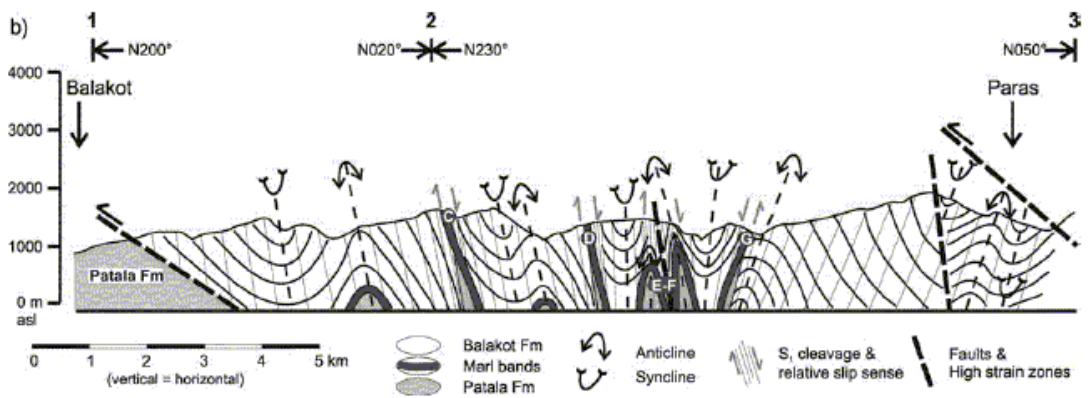
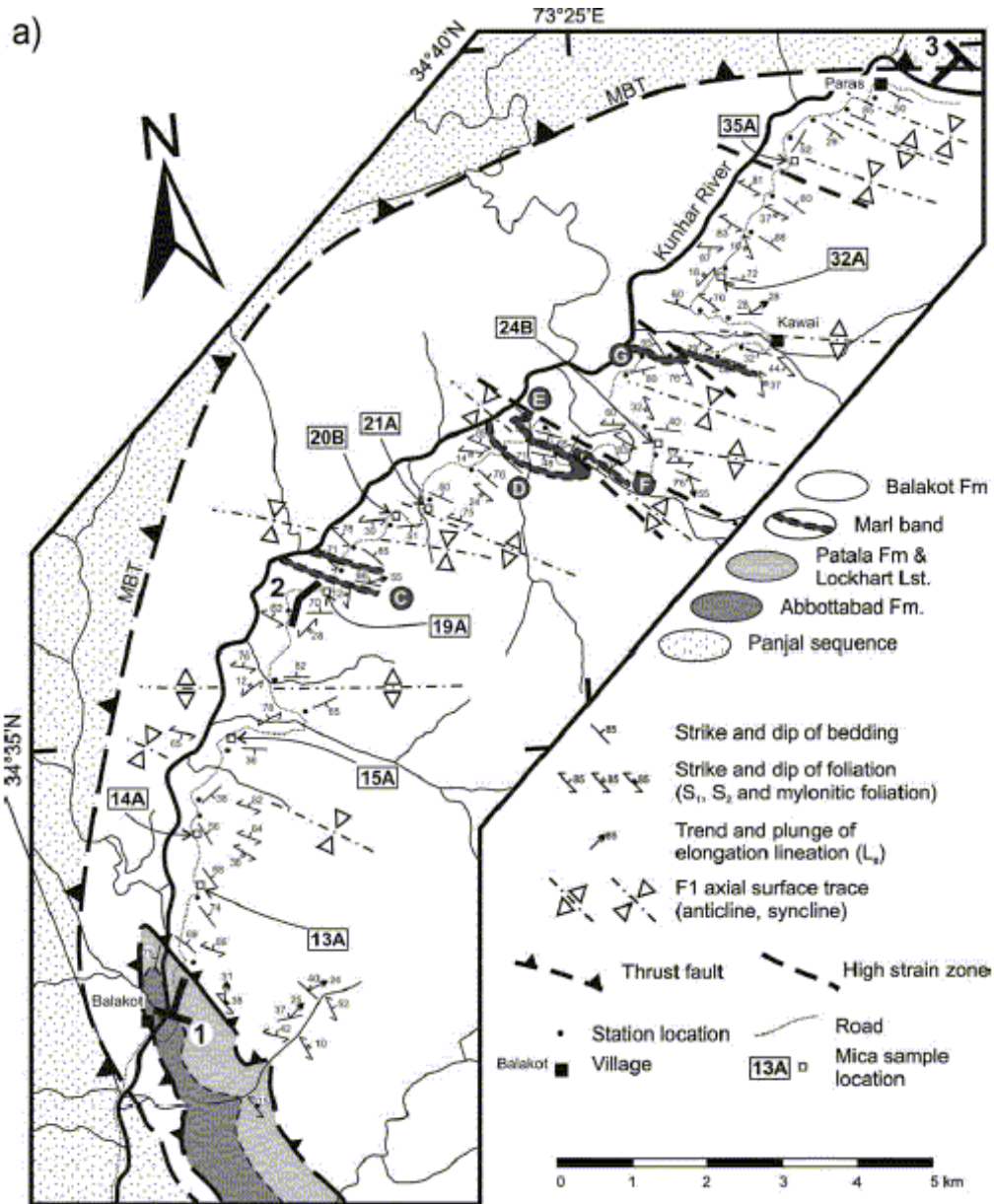


Figure 3.2: A close-up map of geology of the Balakot area

4 TECTONICS

Apparently, about 225 million years ago, the Indian continent was a large island situated off the Australian coast. A vast ocean called the Tethys Sea separated the Indian continent from the rest of the Asian continent. Later when Pangea began to break apart, India began to move northward. About 80 million years ago, India was located just south of the Asian continent, moving northward at a rate of about 9-m a century. Eventually India collided with Eurasia about 40 to 50 million years ago, and its northward advance slowed by about half. The Himalayas are also in continuous motion. They are growing by more than 1cm a year, which is a growth rate of 10 km in a million years. Although due to erosion and some subsidence of the whole area due to gravity, the effect of this growth is distorted. Himalaya mountain range constitutes the northern plate boundary of the Indian plate. Chaman fault in the west and Sagaing fault in the east is the transform plate boundaries. While Chaman fault is a sinistral fault, the Sagaing fault is a dextral fault. The indentation of the Indian plate into Euroasia resulted in the formation of Altyn Dağ (Altyn Tagh) and Karakorum faults in the central Asia (Figure 4.1).

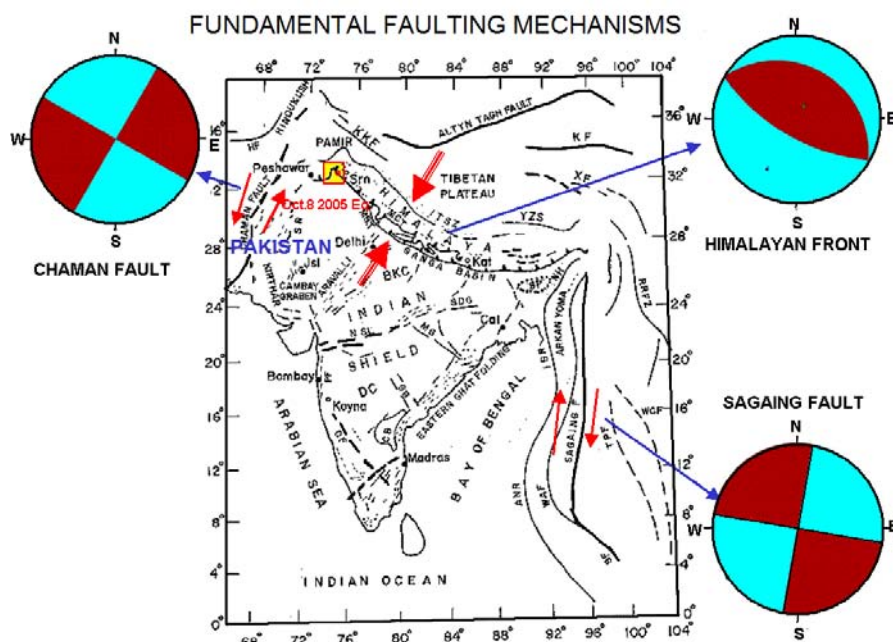


Figure 4.1 Tectonic features of Indian plate and its close vicinity

The Jammu & Kashmir is the western most extension of the Himalayan mountain range in India. Here it comprises of the Pir Panjal, Zaskar, Karakoram and Ladakh ranges. The boundary of the Punjab plain and the mountains forms the Himalayan

Frontal Thrust (HFF), which in this area is the Murree Thrust. The Main Boundary Thrust (MBT) underlies the Pir Panjal Range and is known as the Pir Panjal Thrust in the region. The Zaskar range which are part of the Great Himalayan range are underlain by the Zaskar Thrust. The Kashmir Valley lies between the Pir Panjal and the Zaskar thrusts, making it very vulnerable to earthquakes. Other northern parts of Jammu & Kashmir are heavily faulted. Along the Zaskar and the Ladakh ranges runs a NW-SE trending strike-slip fault, the longest in the Jammu & Kashmir area. The main faults in the epicentral area are Murree fault and Panjal fault. Both of these faults are thrust fault. While Murree fault dips NE, the Panjal fault dips SW. These two faults may be conjugate to each other and they are in the foot-wall side of Main Boundary Fault (MBF).

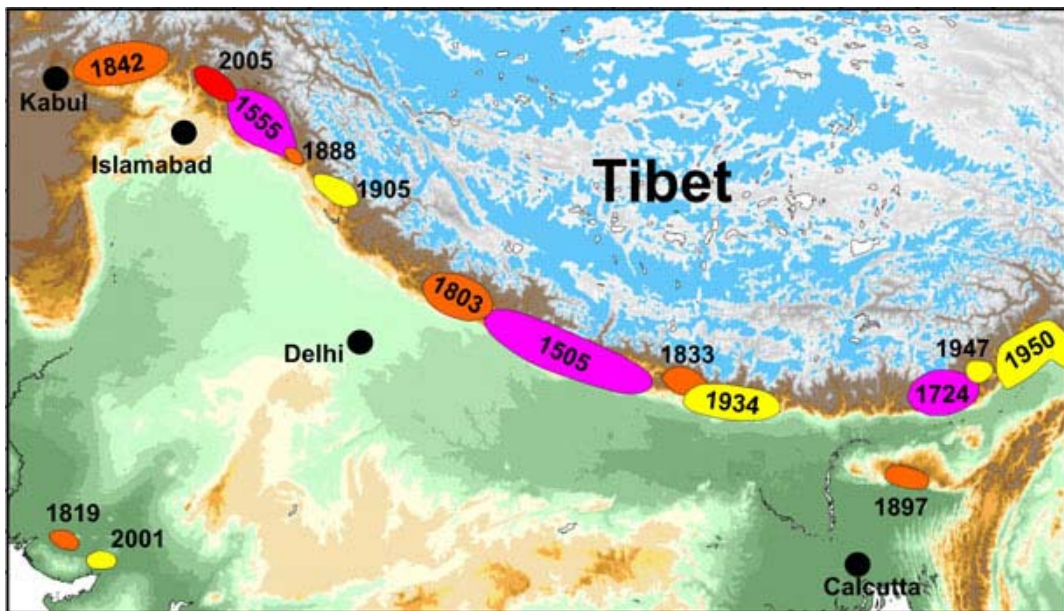


Figure 5.1 Large earthquake events along Himalaya front (from Wright, 2005)

5 SEISMICITY

The historical seismicity of the area was studied by several researchers (i.e. Bilham 1989; Bilham & Ambraseys, 1988, etc.). The earthquakes along the Himalayan front and the areas of their influences are shown in Figure 5.1. In view of the earthquakes shown in Figure 5.1, the Oct.8, 2005 earthquake occurred in a place, which may be regarded as a seismic gap. However, the gap is not fully ruptured and another earthquake having a similar magnitude may rupture in the region between the 1842 earthquake and the 2005. In addition, a seismic gap exist in the north of New Delhi. If the rupture takes place as a single event, it may produce an earthquake of M8 class.

Figure 5.2 shows the pre-post seismicity of the epicentral area using the data base of NEIC between 1973 and 2005. Before the Oct. 8 earthquake, there is almost no earthquake activity in the epicentral area, and a very high seismic activity has been taking place following the main shock. The high seismic activity is concentrated around the NW tip of the causative fault. Figure 5.3 shows the seismicity along a cross section perpendicular to the strike of the causative fault. It is interesting to note that the projections of the shocks imply that the fault plane should have the inclination of 30° .

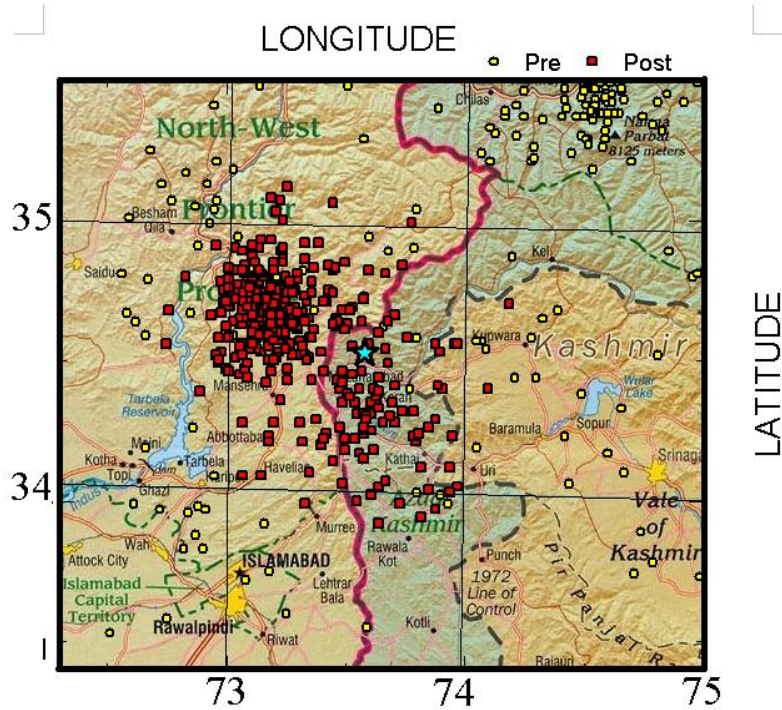


Figure 5.2 Pre-post seismicity of the epicentral area

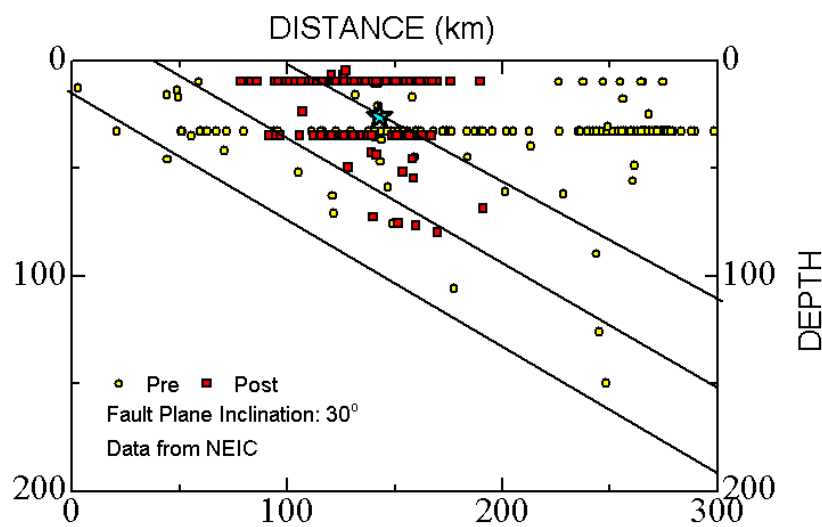


Figure 5.3 Seismicity along a cross-section perpendicular to strike of the causative fault

6 CRUSTAL DEFORMATION AND STRAINS

Crustal deformation measurements have been carried out to observe the motions of crustal plates by International GPS service. Although some local GPS network are used in both Pakistan and India, the measurements are not continuous. Therefore, it is presently difficult to know the local straining and stresses in the vicinity of the earthquake area. A rough estimation of the crustal straining in the vicinity in Pakistan and India is carried out using the measured annual deformation rates of GPS stations, namely, BAHR(Bahreyn), IISC (India), KIT3(Uzbekistan) and LHAS(Tibet). The deformation rates at these stations are given in Table 6.1 and computed strain rates given in Table 6.2. The illustrations of annual deformation rates and strains are shown in Figure 6.1. As noted from the computational results, Indian plate in Pakistan undergoing much higher straining as compared with that of India.

Table 6.1 Annual deformation rates measured

Station	X(E+)	Y(N+)	UD(U+)
BAHR	32.10	28.76	0.94
IISC	42.89	33.66	0.93
LHAS	45.68	12.50	1.93
KIT3	28.02	3.75	-2.0

Table 6.2 Computed Annual strain rates

Element	$\Delta\varepsilon_1$ ($\mu\text{s}/\text{year}$)	$\Delta\varepsilon_3$ ($\mu\text{s}/\text{year}$)	θ (radian)
1	7.45044	-20.1116	-50.0149E-02
2	8.73246	13.3154	-22.4190E-02

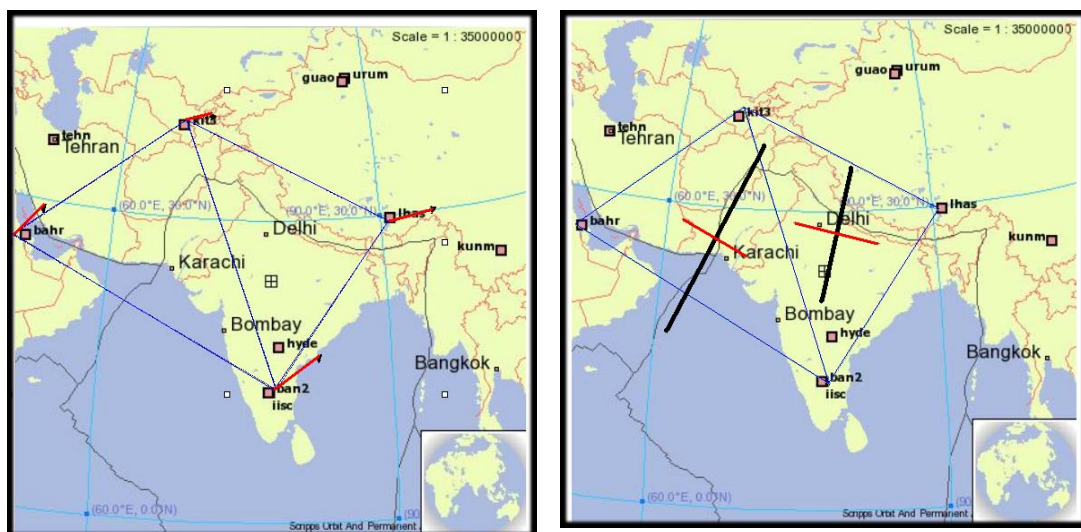


Figure 6.2 Crustal deformation rates and strain rates in the vicinity of Pakistan

7 FAULTING CHARACTERISTICS AND SURFACE DEFORMATIONS

The fundamental parameters of the Oct. 8, 2005 earthquake were estimated by various institutes worldwide and they are listed in Table 7.1. Furthermore, the fault plane solutions are shown in Figure 7.1. Although there are some differences among the parameters of the earthquake estimated by various institutes, the all solutions indicate thrust faulting with a slight lateral component except the one by USGS. As two fault planes are obtained from these solutions, the causative fault should be inferred from additional observations and seismic data. In view of the regional tectonics, after-shock activity, the fault plane dipping to NE should be the causative fault. If NE dipping fault is the causative fault, then the lateral strike-slip component of the faulting implies dextral motion of the fault.

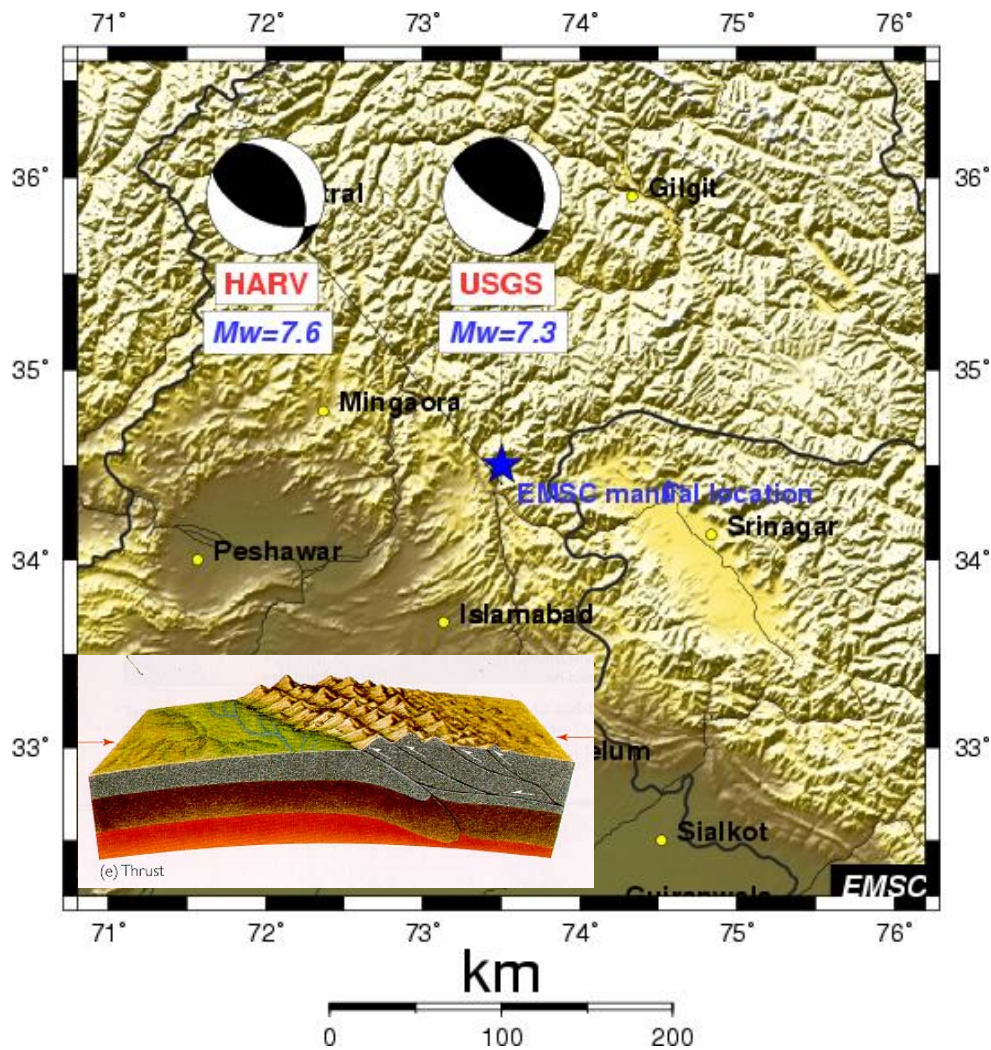


Figure 7.1 Fault plane solutions obtained by various institutes (modified from EMSC)

Table 7.1: Parameters of the earthquake estimated by different institutes

Institute	Latitude	Longitude	Depth (km)	Magnitude	Strike	Dip	Slip
ERI			5	Ms=7.6 Mw=7.6	NP1 326° NP2	29°	108°
BRI	-	-	9	Mw=7.6	NP1 322° NP2 121°	31° 61°	108° 79°
HARVARD	34.37	73.47	12	Mw=7.6	NP1 333° NP2 116°	39° 57°	121° 68°
USGS	34.432	73.537	20	Mw=7.3	NP1 358° NP2 124°	29° 72°	140° 67°
IRD, France			15	Mw=7.7	NP1 318° NP2	29°	107°

Fault rupture propagation was inferred by various institutes such as BRI, IRD, USGS and ERI. The first computational results were released by Yagi of BRI (2005), which were followed by the others. Solutions by BRI, ERI and USGS estimated that maximum slip should be ranging between 8-13m, while the solution by USGS and IRD indicated that the slip should be ranging between 4 to 6m. Furthermore, these solutions indicated that the maximum ground deformations should occur at the ground surface. The empirical relations proposed by Aydan (1997) and Matsuda (1975) infer the relative slip to be 3.2, and 3.6m, respectively. Since there was no surface rupture to confirm these estimations, it is very difficult to make further comments. Nevertheless, the inferred slips by BRI, ERI and USGS are somewhat overestimations.

Japan Geographical Surveying Institute (2005) and Wright-Pathier of Oxford University (2005) inferred the ground displacement using SAR method. The solutions by these two institutes are quite similar to each other. The maximum ground displacements are upward on the hanging wall side of the fault and the amplitude ranges between 4-6m. These values are somewhat close to those inferred from empirical relations and IRD. The inferred trace of the fault is about 80-90km and its NW tip is located in Balakot. The inferred fault trace follows the line Balakot town, Muzaffarabad city and Jhelum valley. Both aerial photographs and land surface observation along this line indicated numerous slope failures. These observations are also similar to the interpretations by Bilham (2005).

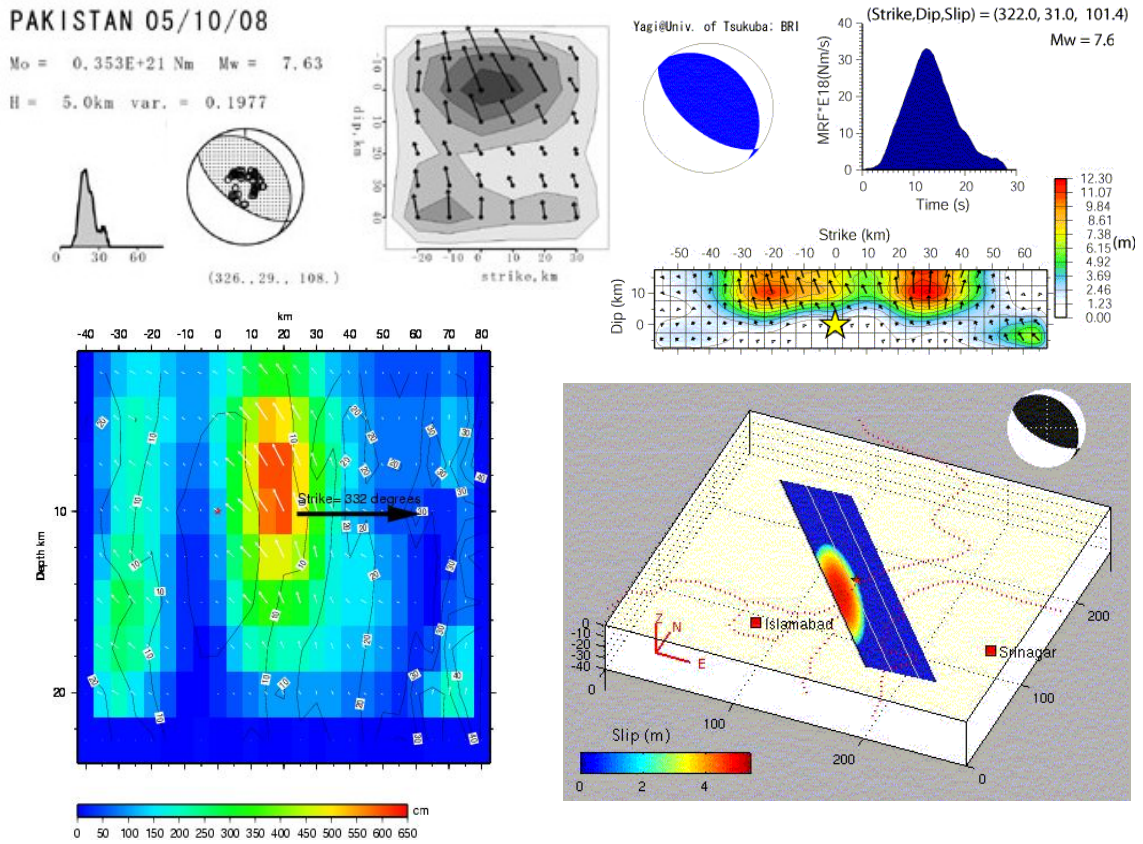
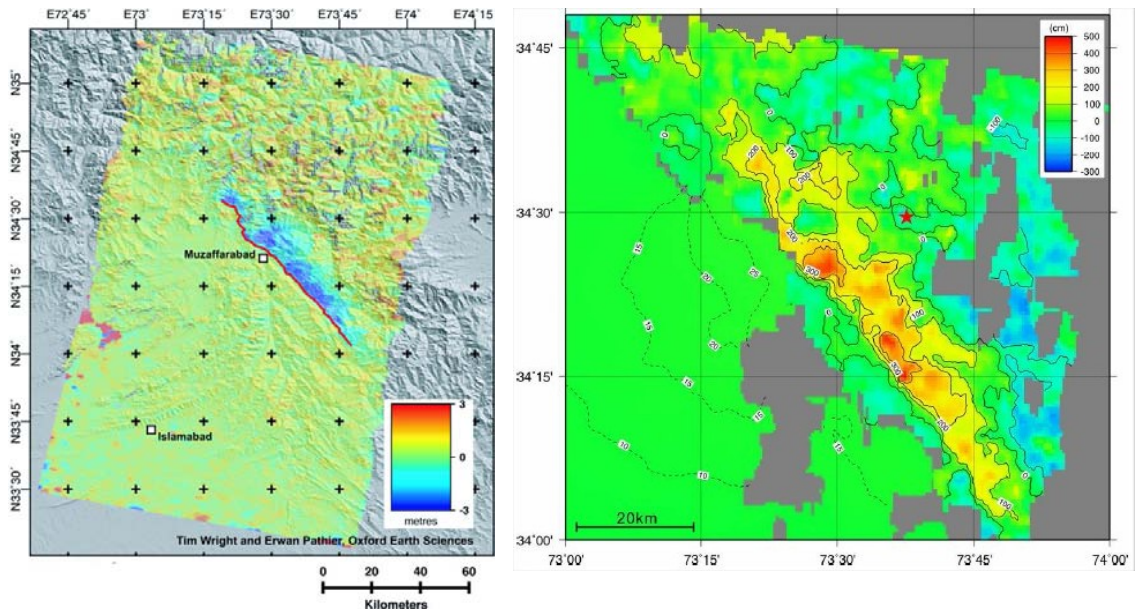


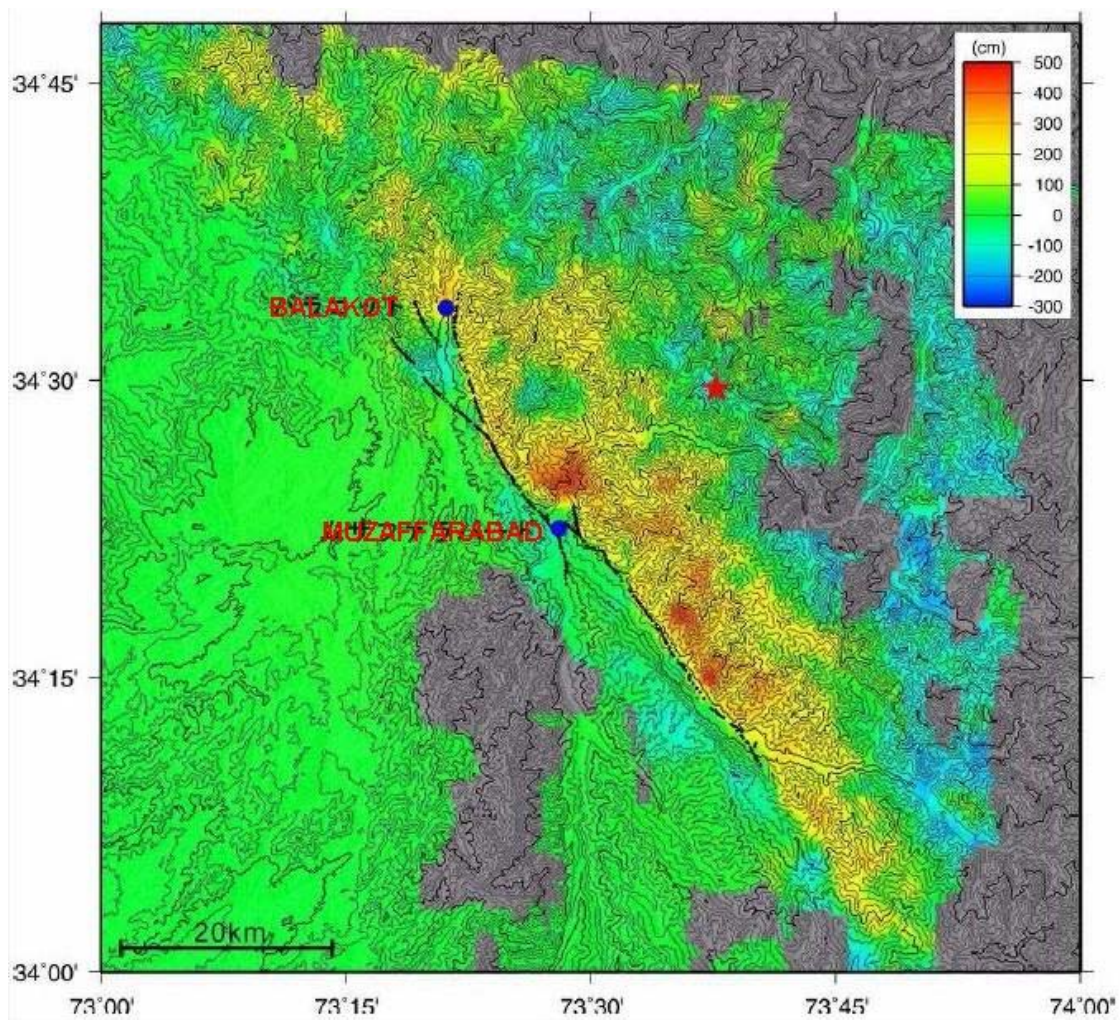
Figure 7.1 Slip distributions inferred by various Institutes



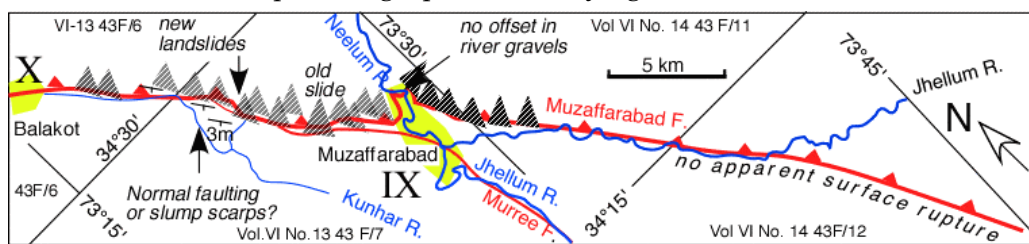
(a) Oxford University (2005)

(b) JGSI

Figure 7.2 Inferred ground surface displacements



(a) Japan Geographical Surveying Institute (JGSI)



(b) Bilham (2005)

Figure 7.3 Inferred fault trace on ground surface

Except a surface rupture observation nearby Bagh by Pakistan Geological Survey (2005), no distinct surface rupture was observed during the investigations in Balakot and Muzaffarabad and Jhelum Valley by the JSCE team. However, there were numerous slope failures particularly on the NE side of the valleys. There were very large scale surficial slope failures in the whitish about 100m thick dolomitic layer,

which is a highly deformed and fractured rock unit (Figure 7.4). Figure 7.5 shows a laboratory test on ground deformation in loose non-cohesive ground during thrust faulting. As noted from the figure, in spite of upward motion of the base-rock, some surficial slope failure (similar to small scale seemingly normal faulting) occur within the non-cohesive deposits. Furthermore, the thickness of deposits increases above the tip of the moving hanging wall as a rigid-body. Therefore the slope failures observed particularly on the hanging-wall side of the fault can be interpreted as the surface expressions of the earthquake faulting.



Figure 7.4 Slope failures observed in the regions of Balakot and Muzaffarabad

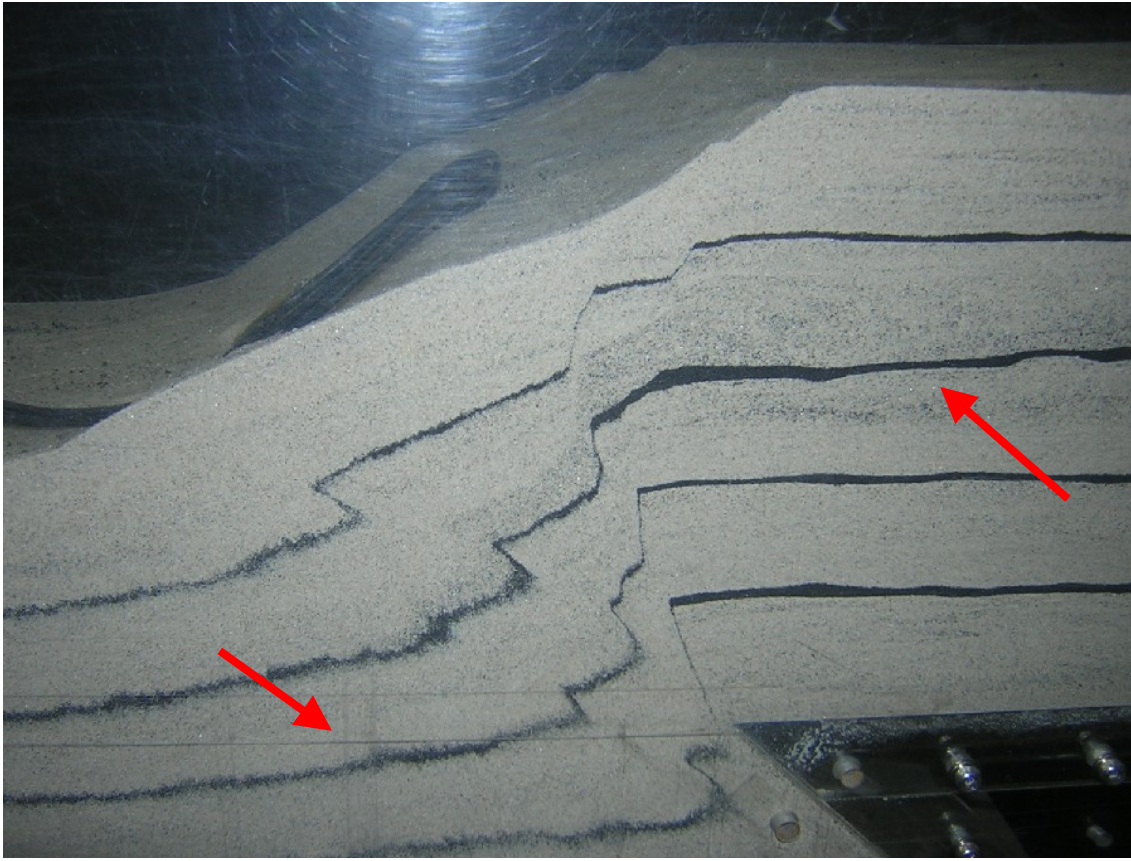


Figure 7.5 A view of non-cohesive deposits over the thrust movement of the basement

Following the main shock, an intensive aftershock activity was observed. Although the aftershocks distributed over a broad area, most of the aftershocks occurred to the north of the main shock. The faulting mechanisms of the aftershocks are shown in Figure 7.6. The faulting mechanisms of most of the large aftershocks are quite similar to that of the main shock.

Figure 7.7 shows the magnitude and cumulative magnitude of post-seismicity as a function of time. The seismic activity tends to decrease gradually. Nevertheless, from time to time, there are some large aftershocks with a magnitude greater than 5.

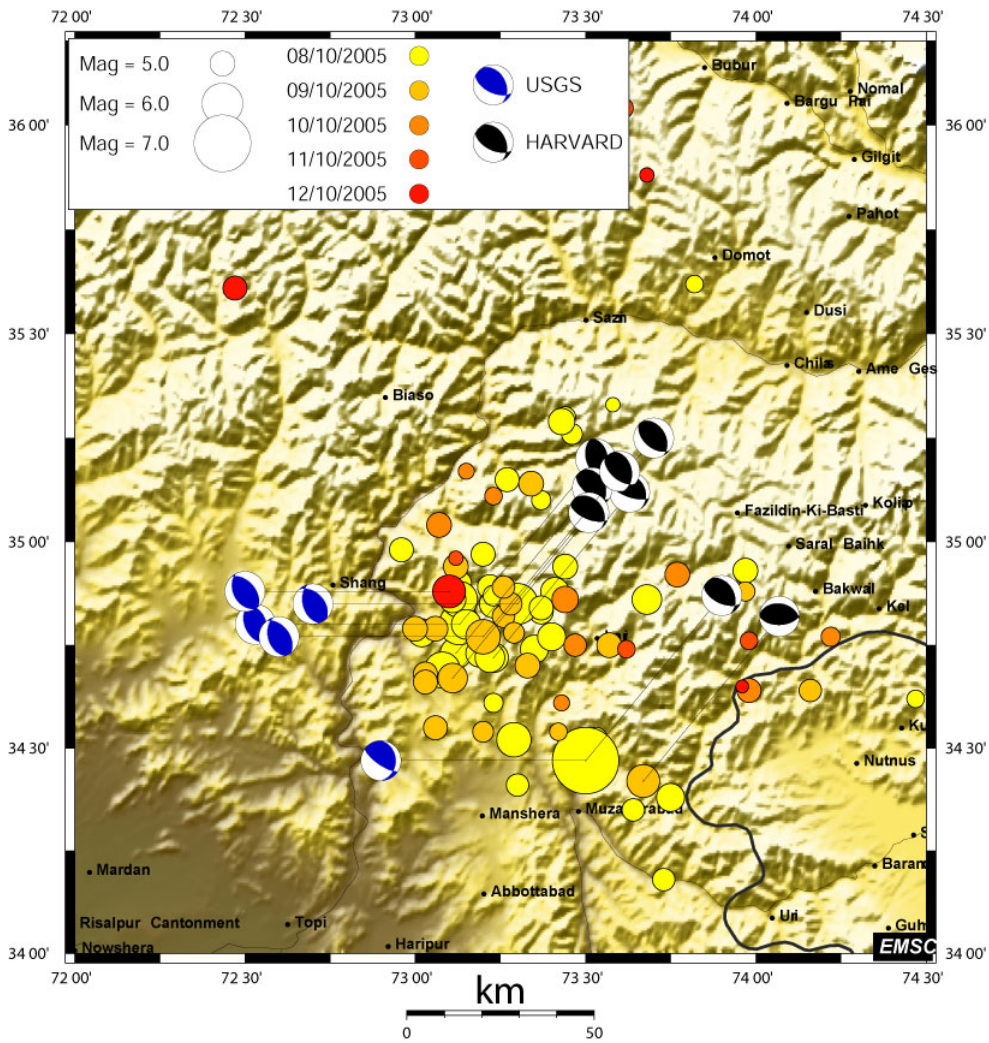


Figure 7.6 Fault plane solutions of large aftershocks

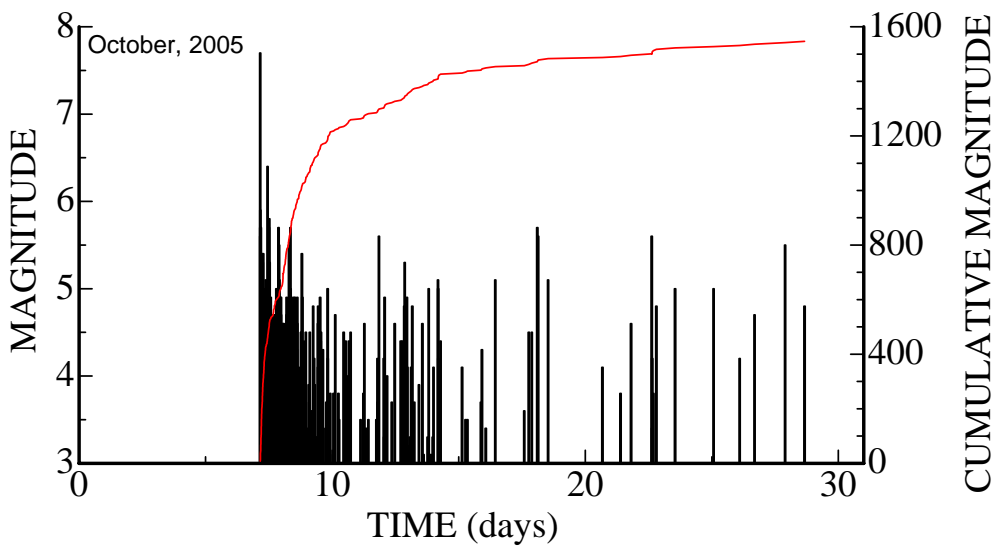


Figure 7.7 Variations of magnitude and cumulative magnitude with time

During the investigations, the striations of the fault surfaces at three different locations were measured (Figure 7.8). In the close vicinity of Balakot on the SW side of the valley, two different faults striations on fault planes having similar orientations were measured. While one of the events indicated thrust faulting (Balakot TF) with slight sinistral lateral component, the other event indicated almost pure sinistral movements (Balakot SSF). It is of great interest that the faulting mechanism of the thrust faulting event at Balakot remarkably similar to the faulting mechanism of the main shock except its lateral component. The other two fault striation measured on the west and east side of the Jhelum valley between Muzaffarabad and Murree. The faulting mechanism for two events are remarkably similar to each other.

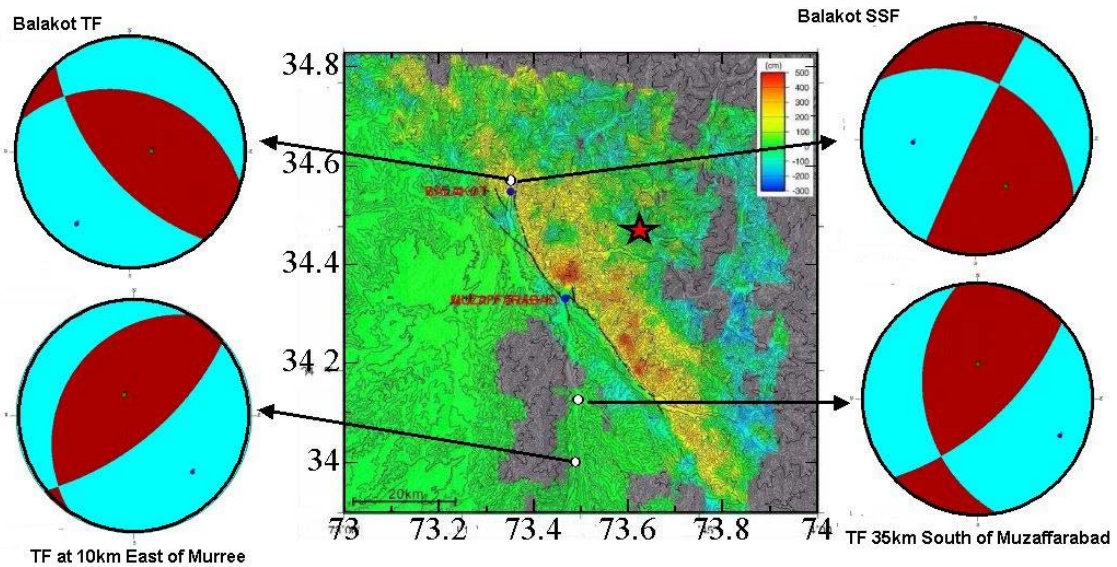
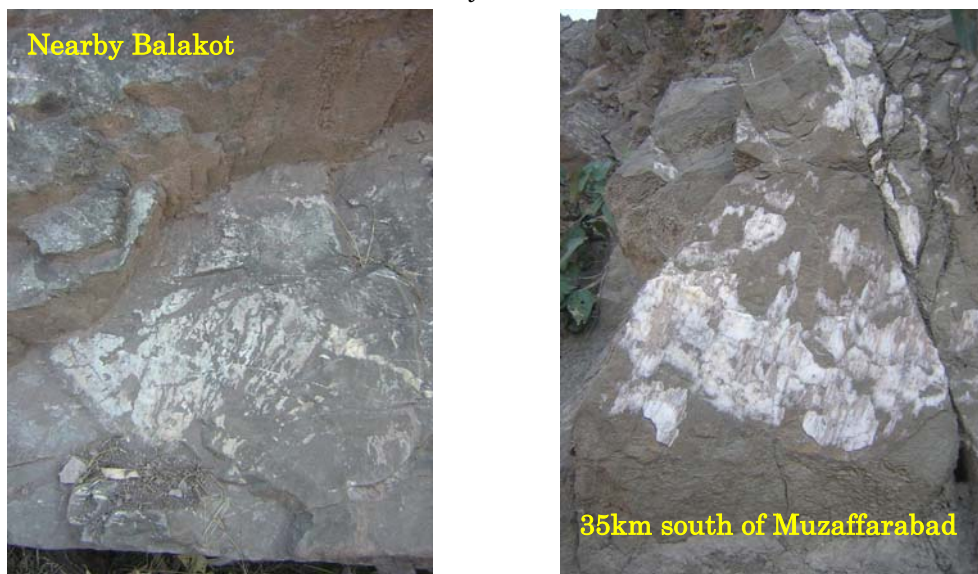


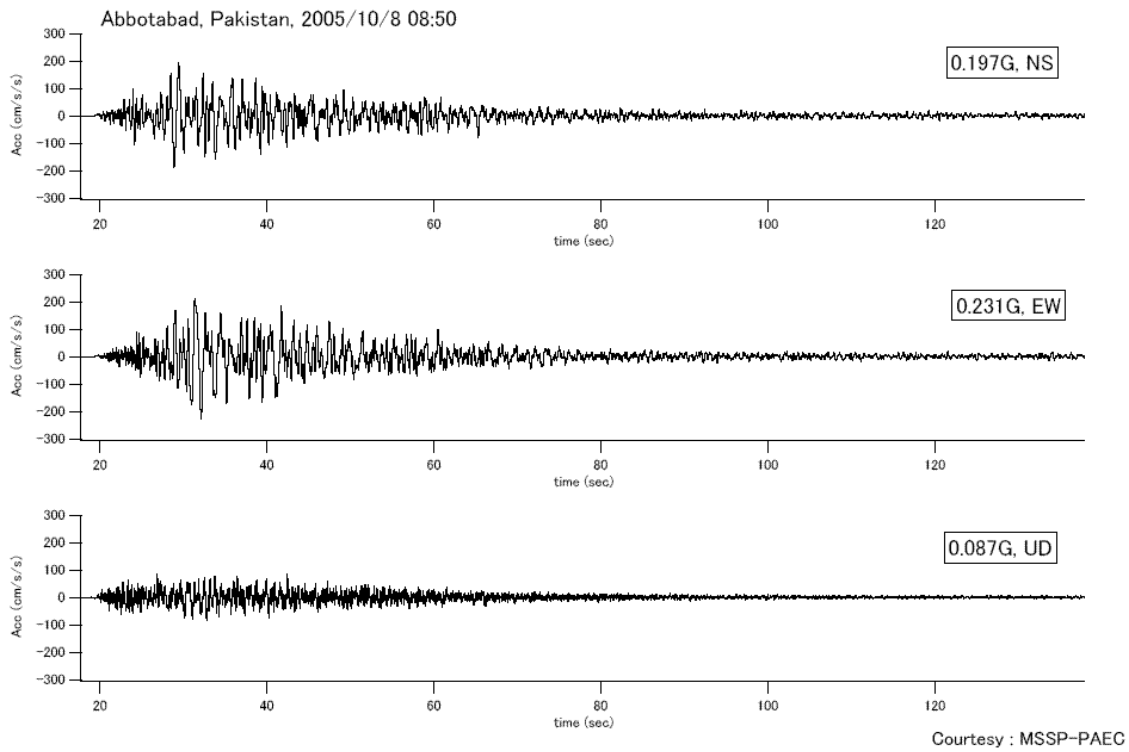
Figure 7.8 Inferred faulting mechanisms from fault striations in the epicentral area

8 STRONG MOTIONS AND THEIR CHARACTERISTICS

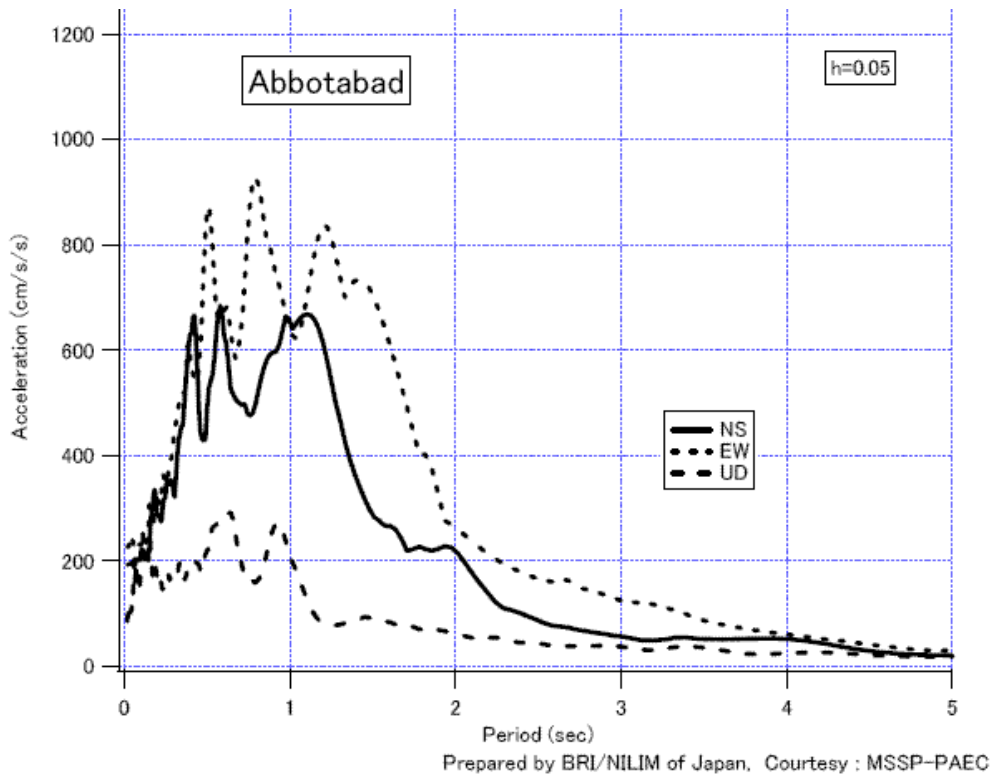
There are several strong motions networks operated by different institutes in Pakistan. The institutes are Pakistan Metereological Agency, Pakistan Geological Survey and Paksitan Atomic Energy Center. The strong motions records for three stations of Micro Seismic Studies Program (MSP) supported by Building Research Institute (Japan) for Pakistan are only available (Okawa, 2005) (Figures 8.1-8.4). The locations of recording stations are Abbotabad, Murree and Nilore. The instruments are situated in some buildings so that they are not free field records. The Abbottabad instrument is located in a small room constructed on alluvium. Murree instrument is inside of a room (ground floor) of two storey building built on steep slope. Nilore instrument is placed in basement of single storey building constructed on sand stone. The Nilore station is a two room structure with a size of about 9m x 14m and height of 5m with the equipment placed on raft of about 1m. The JMA instrumental Intensities were computed as 5.6, 4.4, and 3.7 for Abbottabad, Murree and Nilore, respectively.



Figure 8.1 Locations of strong motion stations

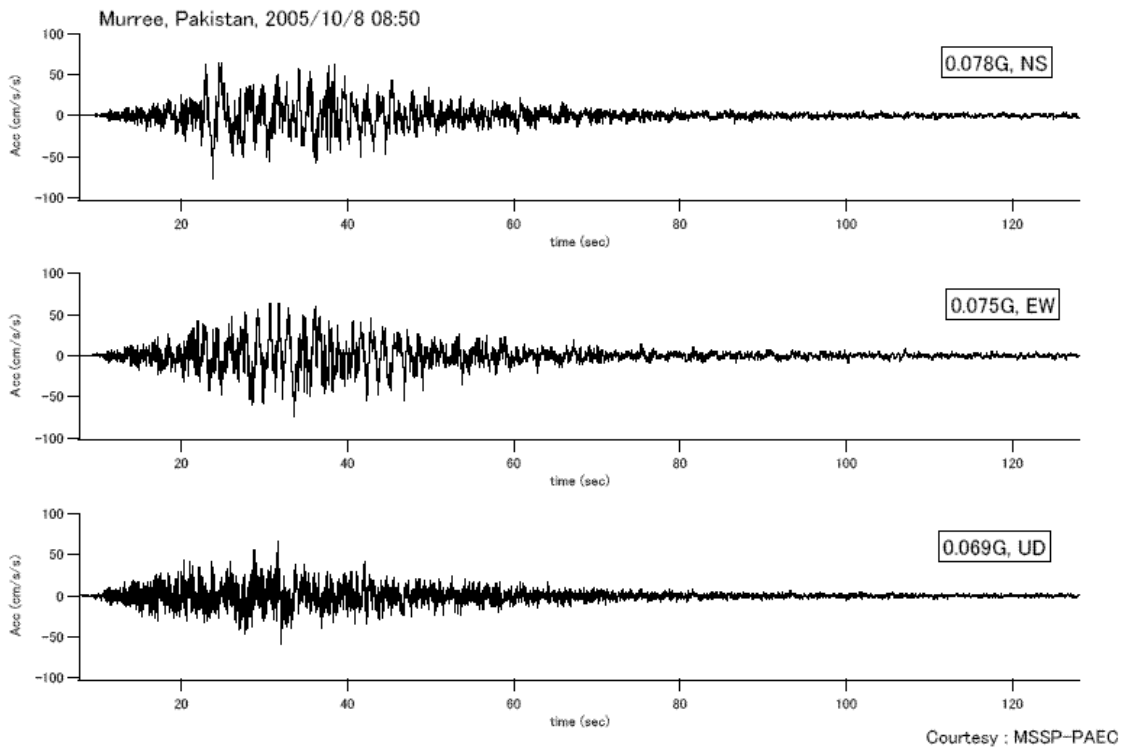


(a) Acceleration records

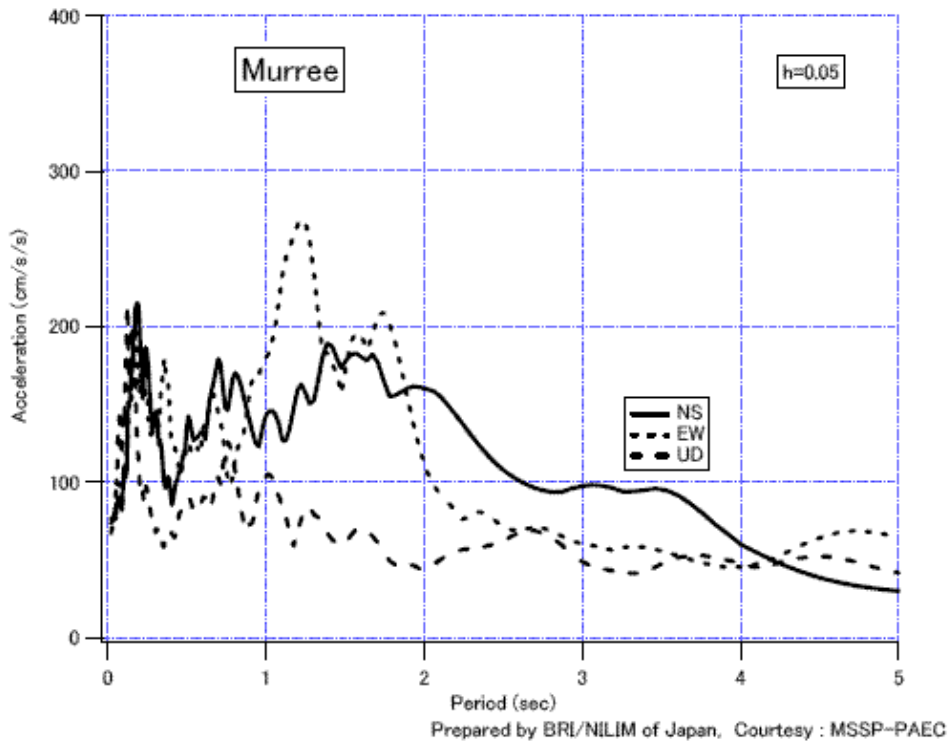


(b) Acceleration response spectra

Figure 8.2 Acceleration records and their acceleration response spectra at Abbotabad

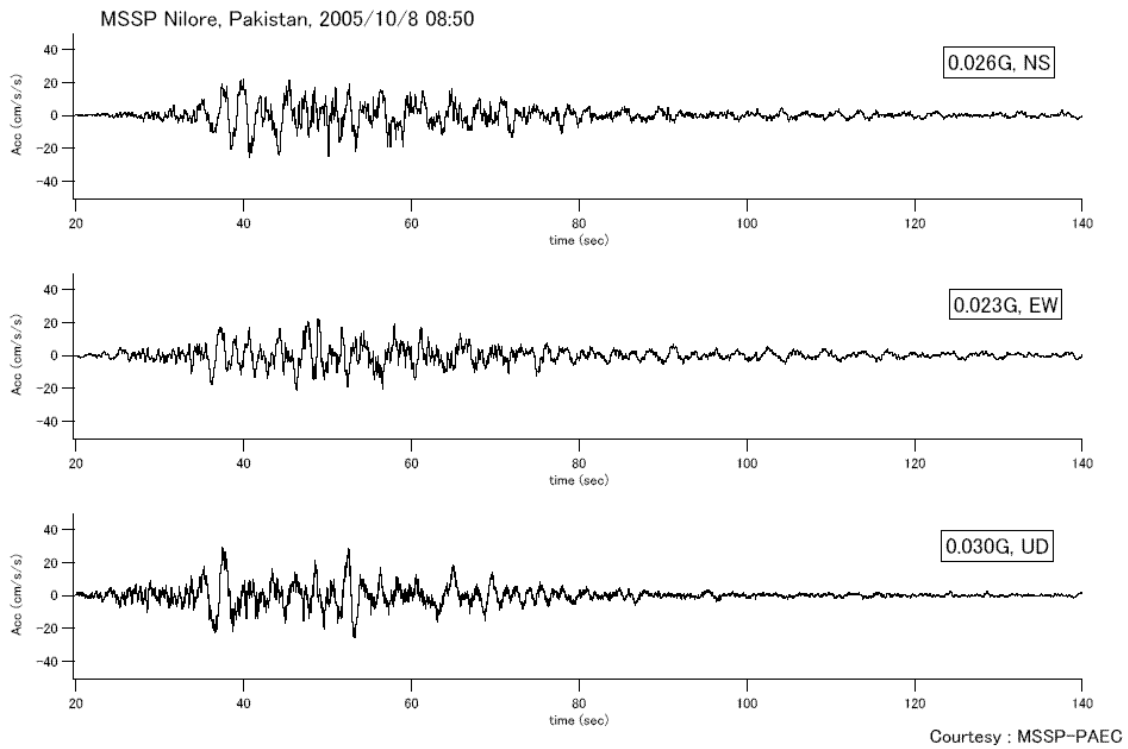


(a) Acceleration records

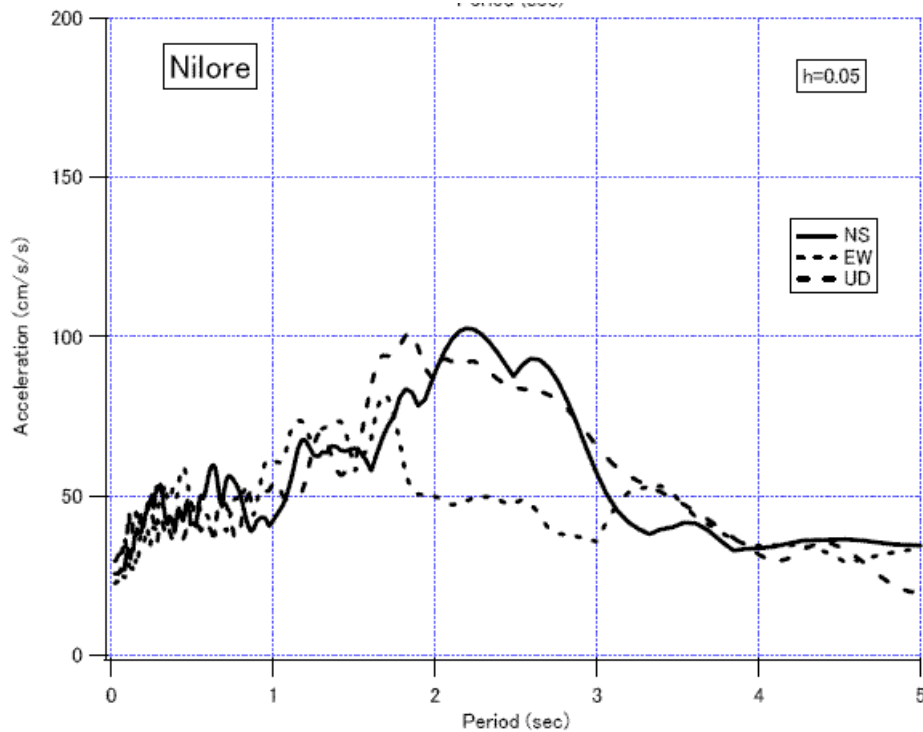


(b) Acceleration response spectra

Figure 8.3 Acceleration records and their acceleration response spectra at Murree



(a) Acceleration records



Prepared by BRI/NILIM of Japan, Courtesy : MSSP-PAEC

(b) Acceleration response spectra

Figure 8.4 Acceleration records and their acceleration response spectra at Nilore

The nearest station to the epicenter is Abbotabad and its response spectra is very flat for the natural period of 0.5 and 1.5s. As the distance increases, the longer period components become dominant as observed in Nilore record. Murree strong motion is situated nearby the peak of the mountain and its response is likely to be influenced by the geometry and structure of the mountain. Compare with records of Abbotabad and Nilore stations, it seems that there is also a dominant natural period of about 0.2-0.25s. The acceleration record of a strong motion station on alluvium ground in Islamabad (according to the statement of an official from PAEC) is about 90gal. Since Nilore is nearby Islamabad, the ground amplification in Islamabad seems to be 3 times that on the bed-rock.

Figure 8.5 compares the observed maximum ground acceleration at three stations as a function of MKS Intensity together with some observations from past earthquakes. The maximum ground acceleration for Balakot was inferred from overturned vehicles. This probably represents the largest ground acceleration in the epicentral area. Balakot is situated on the hanging-wall side of the causative fault. The attenuation of observed maximum ground accelerations are compared with some empirical attenuation relations in Figure 8.6.

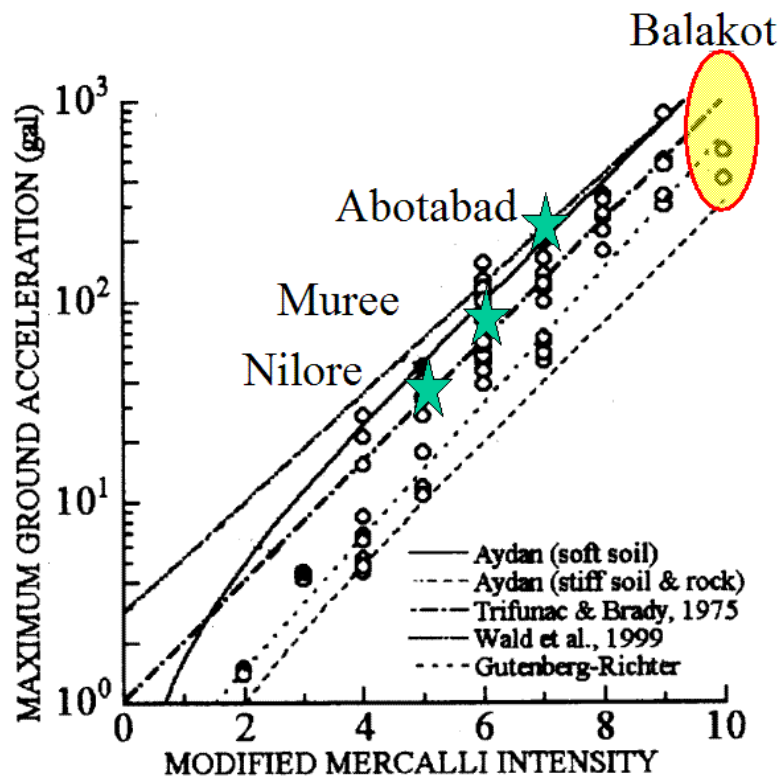


Figure 8.5 Comparison of observed maximum ground acceleration empirical relations as a function of MKS intensity scale (base figure from Aydan, 2001)

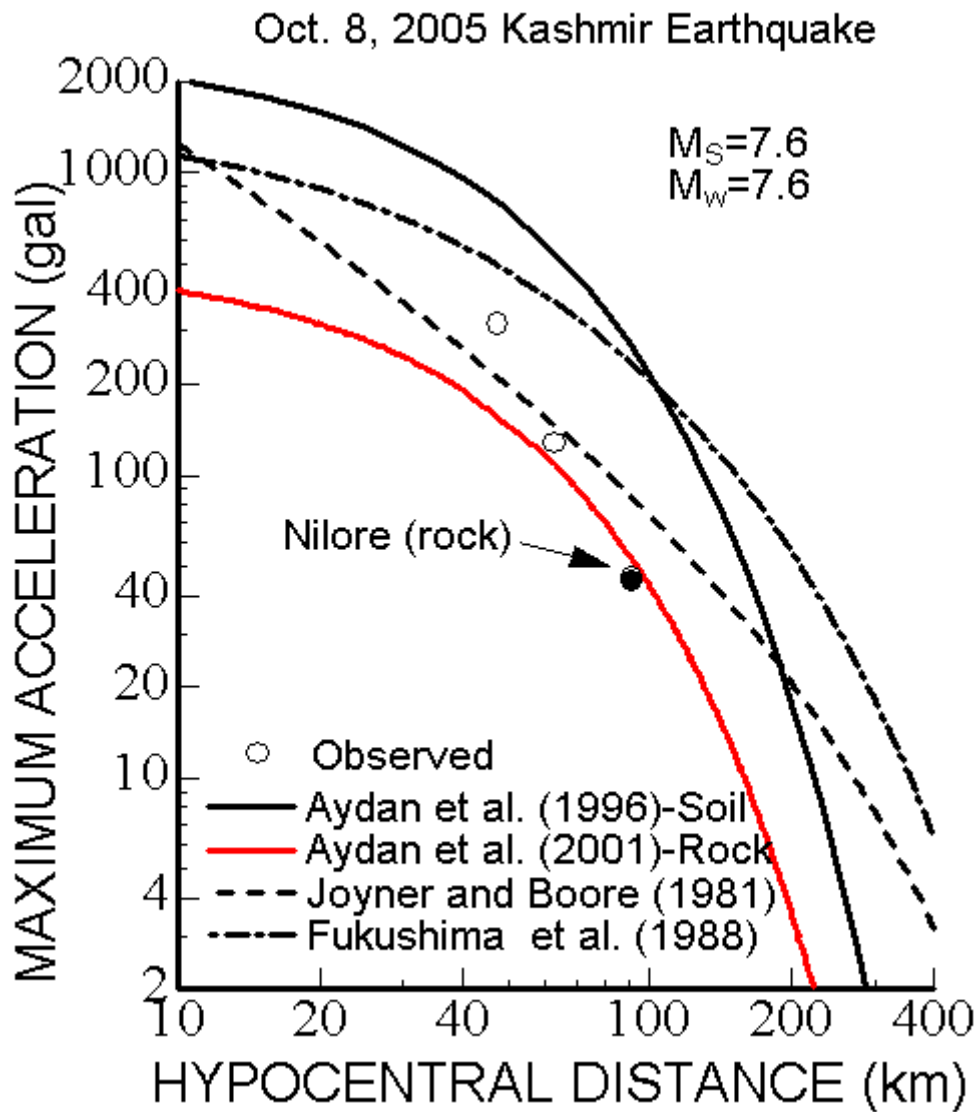
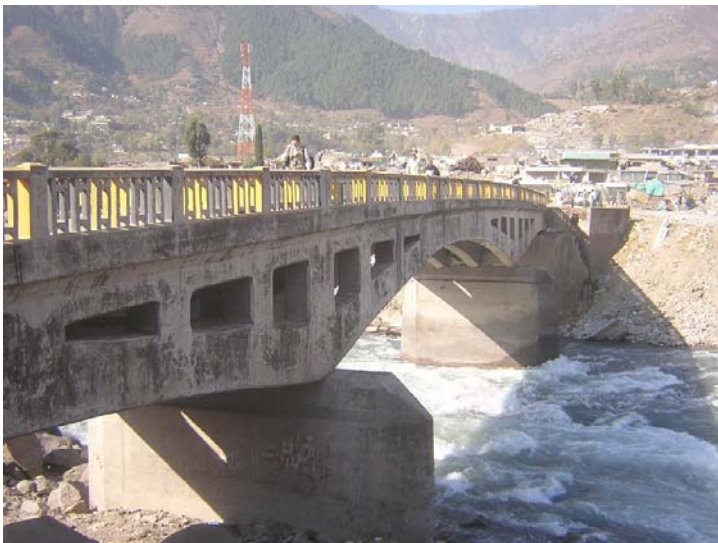


Figure 8.6 Comparison of observed maximum ground acceleration with some of empirical attenuation relations

9 DAMAGE TO CIVIL ENGINEERING STRUCTURES

9.1 Damage to Bridges

There are three bridge types in the epicentral area. Old bridges are either stone arch masonry bridges or truss bridges. New bridges are mainly cast-in place concrete bridges. Heavily damaged bridges observed in valleys running parallel to the strike of the causative fault. Furthermore, the longitudinal axis of the damaged bridges were parallel or sub-parallel to the slip direction of the fault. The largest damaged bridge is located in Balakot town, where the NW tip of the causative fault terminated (Figure 9.1(a)). The axis of the bridge is N38E. The girder of the bridge was displaced about 1m in the SE direction. While the SW side of the bridge sits over the pier beneath, the NE side of the bridge is offset from the pier by about 35-50cm. In other words, it seems that the distance between the piers decreased. The ground on the NE side of the bridge is likely to experience the permanent displacement of ground resulting from the slope failure as well as from faulting. There is no doubt that the inferred ground motion is quite at Balakot and this may also cause the permanent displacement of the bridge deck as the girders was not fixed against horizontal ground motions. Nevertheless, the pedestrian suspension bridge to the south of this bridge experienced compression in its longitudinal axis as seen in Figure 9.1(b), besides its ancors blocks toppled down and the abutment was translated in the SW direction by about 10-20cm. In the same valley, there was another non-damaged RC bridge, whose longitudinal axis is parallel to the valley axis and it is about 2km far away upstream from the damaged Balakot bridge.



(a) RC Balakot Bridge



(b) Suspension bridge

Figure 9.1 Damaged bridges at Balakot



(a) RC bridge with masonry abutments



(b) Damaged masonry arch bridge



(c) Damaged RC bridge with masonry abutments

Figure 9.2 Damaged bridges in Jhelum valley

Several bridges in Jhelum valley between Muzaffarabad and Chakoti route were damaged. Damage to bridges was mainly caused by the collapse or permanent movements of masonry abutments as seen in Figure 9.2.

The bridges in Muzaffarabad city were non-damaged. The bridges about 2-3km away from the causative fault and they are on the foot-wall side of the fault. The Domel bridge is quite old with masonry abutments and single lane truss deck. There is a new RC bridge founded on group pile foundations next to the Domel bridge and they were all non-damaged in spite of high ground motions. However, a pedestrian suspension bridge to the north of Muzaffarabad city, where whitish rock slope failures observed, was collapsed (Figure 9.3). The causes of the collapse are thought to be similar to those of the Balakot bridge.



(a) Satellite images of the collapsed pedestrian bridge before and after the earthquake



(b) Collapsed pedestrian bridge

Figure 9.3 Satellite and land views of the collapsed pedestrian bridge.

9.2 Damage to Roadways and Embankments

Damage to roadways was mainly caused by slope and embankment failures and rock falls (Figure 9.4). The damage to the pavements of roadways by ground shaking could not be observed. The largest roadway damages were observed along highways between Murree and Muzaffarabad and it was about 48km from the USGS epicenter (Figure 9.4(a)). The damage was caused by the embankment failure in a circular sliding failure mode. About 100m long section of the roadway sank more than 15m. The ground consisted of debris of weathered shale and the layers are inclined parallel to the sliding direction (Eastward) of the embankment. The embankments of roadways between Muzaffarabad and Murree, and Muzaffarabad and Chakoti were failed at numerous locations (Figure 9.4(b)). Slope failures and rockfalls obstructed highways. Rockfalls were wide-spread all over the epicentral area.

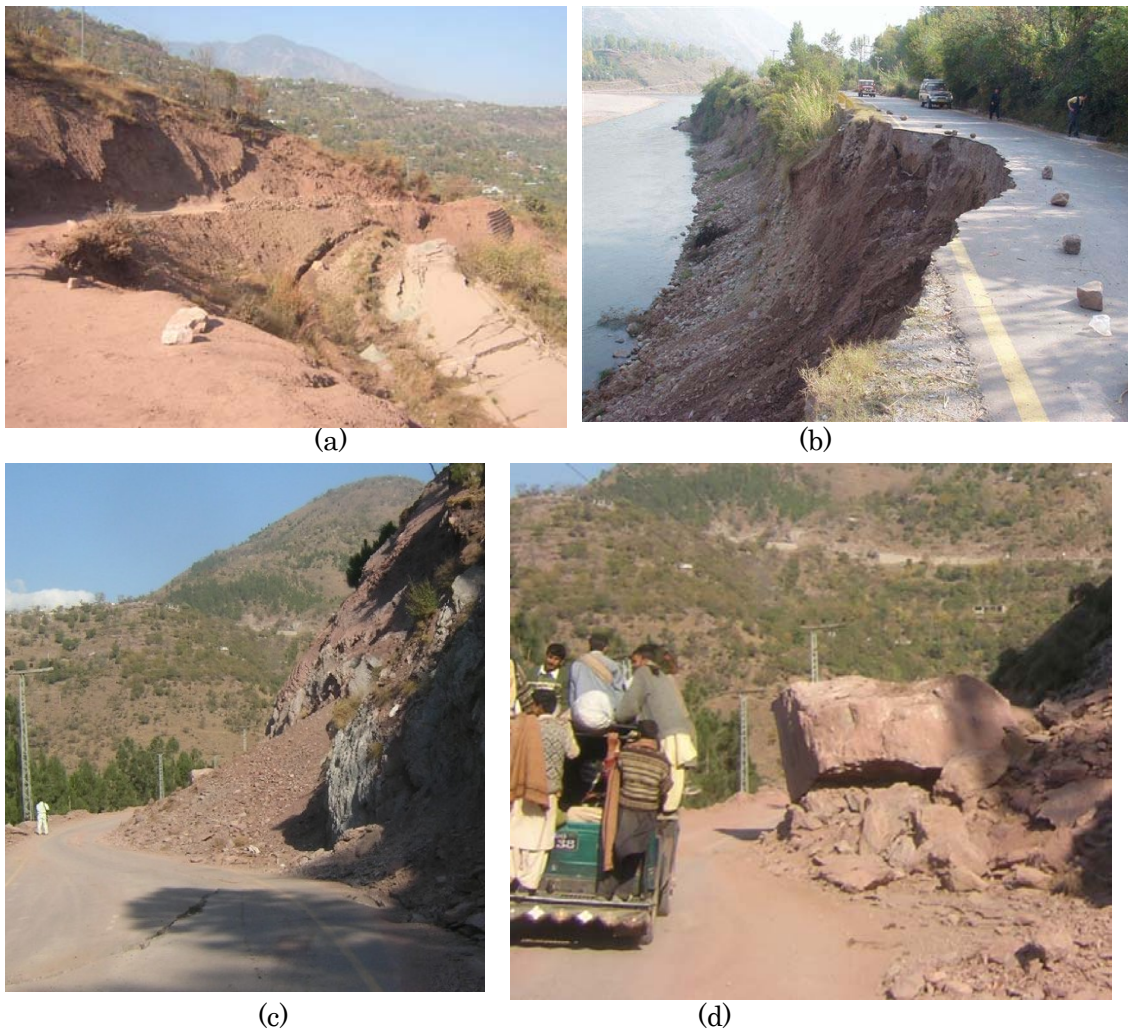


Figure 9.4 Damage to roadways

9.3 Damage to Tunnels

The only tunnel in the epicentral area is located about 4km south of Muzaffarabad. The tunnel is lined with stone masonry lining and it is excavated in shale with an overlaying non-cemented conglomeratic deposit. The south portal of the tunnel was lightly damaged by the slope failure of overlaying conglomeratic deposit as seen in Figure 9.5.

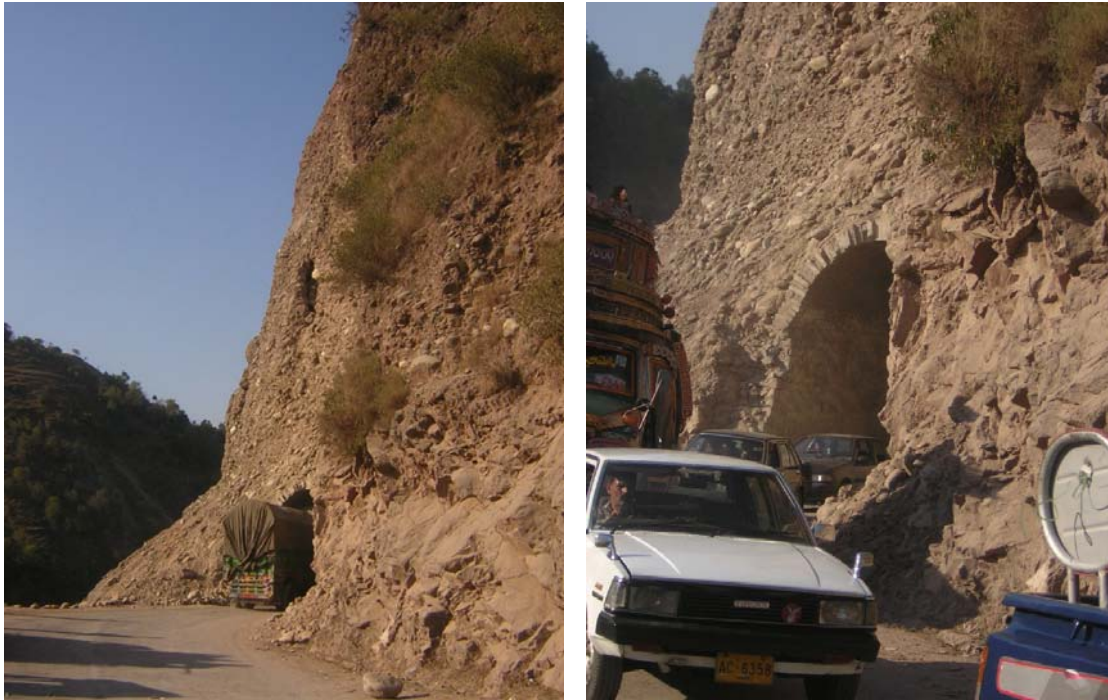


Figure 9.5 Lightly damaged roadway tunnel

9.4 Damage to Pylons and Poles

Damage to pylons and poles were either caused by slope failures or faulting. The most severe damaged observed on NE side of the valley nearby Balakot. Figure 9.6 shows the damaged pylons. The damage to pylons were caused by the uplift of ground and the pylons were all tilted. At this particular location, at least 6 pylons were tilted.

9.5 Dams

The nearest dam to the epicenter is Terbela Dam built for hydroelectric power and also for irrigation. There was no report of damage to this dam (Figure 9.7).



Figure 9.6 Damage to pylons and poles



Figure 9.7 Terbela dam

10 SLOPE FAILURES

One of the most distinct characteristics of 2005 Kashmir earthquake is the wide-spread slope failures all over the epicentral area. Slope failures may be classified in three categories as follows (Figure 10.1):

- a) Soil slope failures
 - Circular Sliding
 - Planar Sliding
- b) Weathered rock slope failures
 - Surficial Slides (common)
- c) Rock slope failures
 - Curved Shear Failure (rare)
 - Planar Sliding
 - Wedge sliding failure
 - Flexural or Block Toppling
 - Buckling Failure

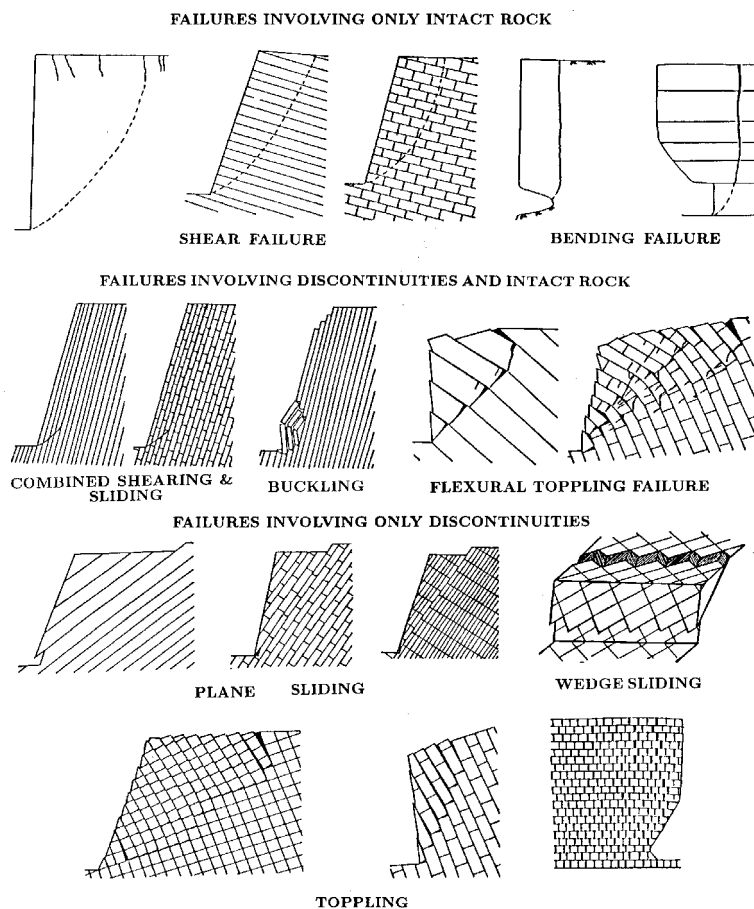


Figure 10.1 Classification of slope failures

10.1 Soil Slope Failures

Soil slopes failures occurred in either plane sliding mode or circular sliding. Planar sliding modes are generally observed on soil slopes over the bed-rock (Figure 10.2(a)). Deep-seated circular type soil slope failures observed when the soil thickness was large. Figure 10.2(b) shows one example nearby Balakot. There were several scarps indicating several circular type slip surfaces within the slope. However, the close inspection of this slope indicated some failures and movements had already took place long before the earthquake.



(a) Planar sliding of soil slope nearby Balakot



(b) Deep-seated circular sliding

Figure 10.2 Soil slope failures nearby Balakot

Some peculiar soil slope failures were observed in both Balakot and Muzaffarabad (Figure 10.3). These slope failures occurred in conglomeratic soil deposits with rounded large cobbles. Since the slope angles were quite steep (70-80°), these slopes failed on planes involving partly vertical tensile cracks and curved shear plane. The residual slope angles (repose angle) ranges between 40-45°, which may be considered to be equivalent its friction angles. Some needle penetration tests were carried out at both Balakot and Muzaffarabad. The cohesion of soil matrix of the conglomeratic soil deposit is inferred from the needle penetration index tests to be ranging between 60-100 kPa.



(a) Muzaffarabad



(b) Balakot

Figure 10.3 Soil slope failures at Muzaffarabad and Balakot

10.2 Weathered Rock Slope Failures

Rock units in the epicentral area are schists (phyllite-like), sandstone, shale, limestone and dolomite. Particularly red shale of Balakot formation is prone to weathering and the thickness of the weathered rock seems to be about 2-5m. Dolomitic rock unit is intensively sheared and this unit is thought to be constituting the fault fracture zone. Figure 10.4 shows a surficial slope failure in weathered red shale nearby Balakot. The surficial slope failures in dolomitic rock unit was spectacular and continued for several kilometers as they are clearly noticed in satellite images (Figure 10.5 and Figure 10.6)

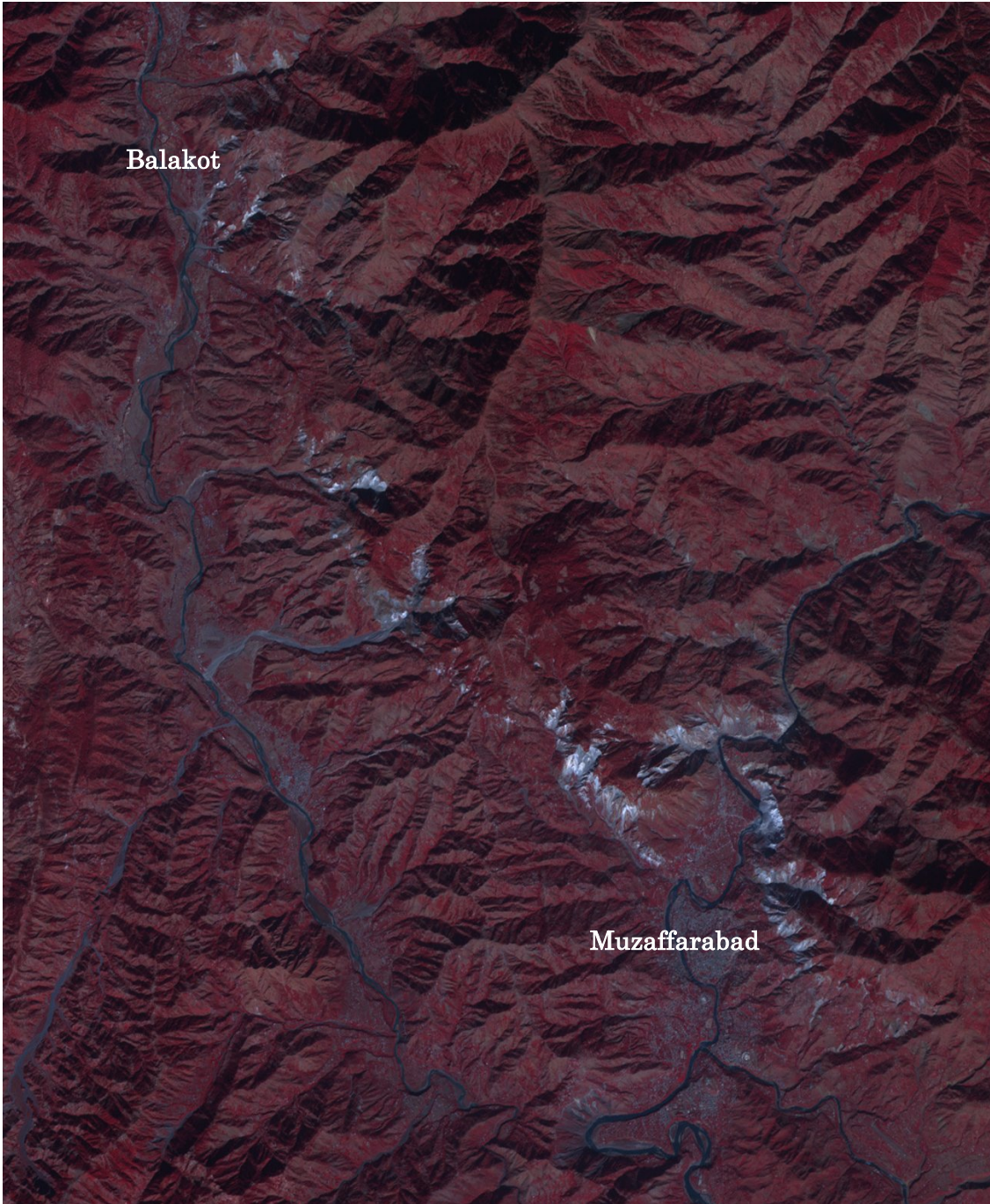


(a) Nearby Balakot



(b) Muzaffarabad

Figure 10.4 Surficial slope failures in weathered or fractured rock



(Whitish areas are surficial slope failures in intensively sheared dolomitic rock unit)
Figure 10.5 Satellite image of surficial slope failure in intensively sheared dolomitic rock unit

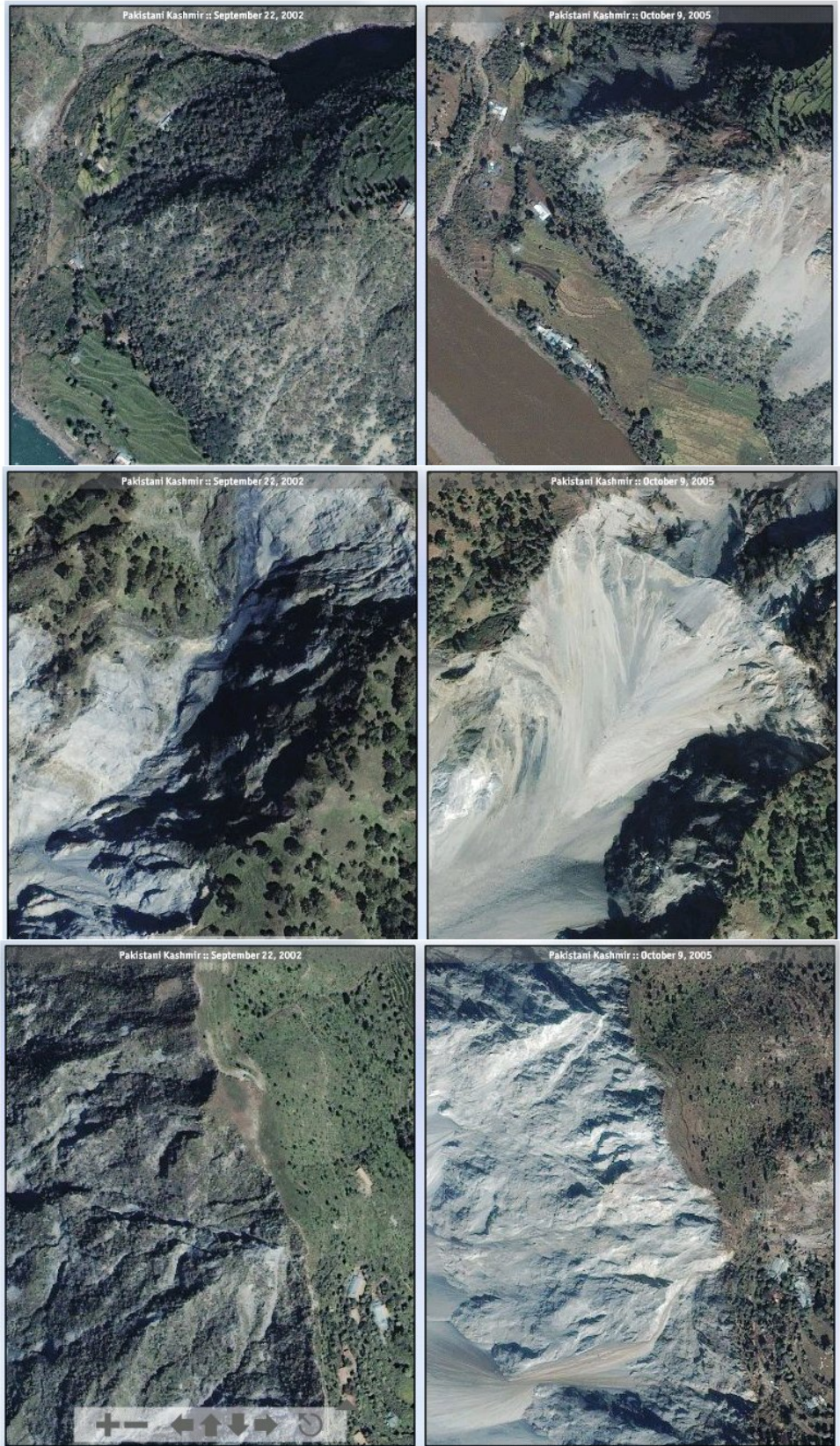


Figure 10.6 Satellite images of slope failures nearby Muzaffarabad

10.3 Rock Slope Failures

Rock units are schists (phyllite-like), sandstone, shale, limestone and granite. Except granite, all rock units have at least one throughgoing discontinuity set, namely, bedding plane or schistosity plane. Since rock units had been folded, they also include joint sets and fracture planes as a result of tectonics movements. Granite also has at least three discontinuity sets. In regard with rock slope failures classified in Figure 10.1, the rock slope failures are mainly planar sliding, flexural or block toppling failure. Planar sliding failures were observed mainly in schists, sandstone and shale while flexural toppling failure was observed in intercalated sandstone and shale (Figures 10.7 & 10.8). The inclination of layers ranges between 30-65°, which implies the sliding failure can be easily caused by a small intensity of disturbing forces resulting from such as earthquakes, heavy rainfall or the both.



Figure 10.7 Some examples for planar sliding failure of rock slopes

Rockfalls in the epicentral area generally resulted from the toppling of rock blocks due to excitation of the earthquake. Numerous rockfalls were observed for a great length of roadways. Rockfalls were common in sandstone slopes. Some flexural slope failures were also observed in intercalated sandstone and shale formation with undercutting.



(a) Rockfalls



(b) Flexural toppling failure

Figure 10.8 Some examples of block or flexural toppling failure of rock slopes

The satellite images indicated that there was a large scale slope failure in the vicinity of the SE tip of the causative fault (Figure 10.9). Although the area could not be visited by the JSCE team, the slope failure may be of planar sliding or asymmetric wedge sliding

type. This type sliding generally observed on rock slopes having layers dipping towards to free slope surface.

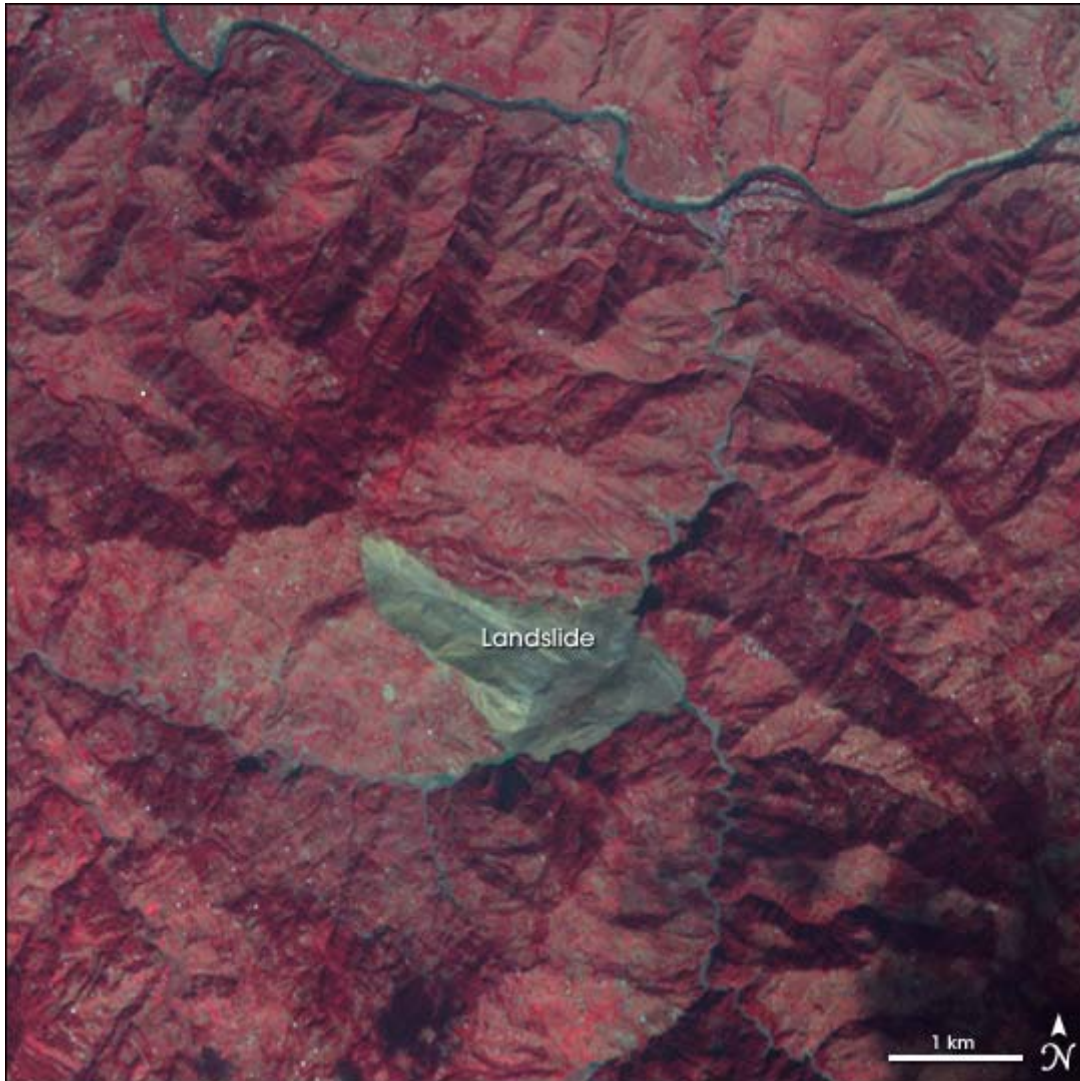


Figure 10.9 A large scale slope failure detected from a satellite image

11 RECOMMENDATIONS FOR REHABILITATION AND RESTORATION

Recommendations for the rehabilitation and restoration of bridges, roadways, embankments and slopes are described in this chapter. Recommendations are concerned with temporary and permanent measures.

11.1 Recommendations for Bridges

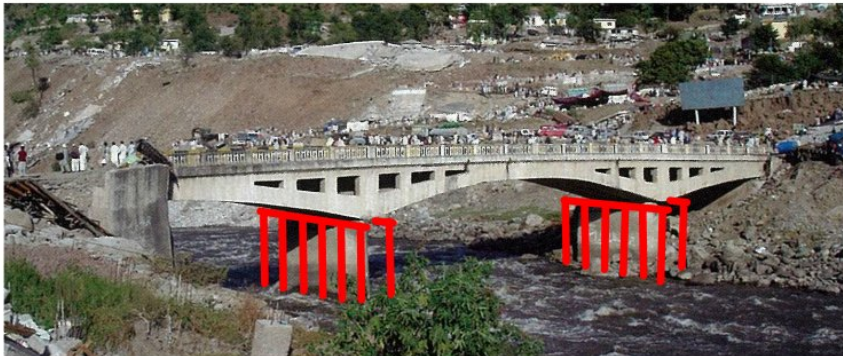
There are several severely damaged bridges in the epicentral area. The most severely damaged largest bridges were in Balakot town. Balakot Bridge is a 3 span girder bridge. The girder of the bridge is displaced laterally for about 1m downstream side and the NE side of the bearings are offset from the pier. Furthermore, the concrete of the girder is damaged at several locations. Damage to the cross beam of the superstructure is found to be relatively severe while the damage to main girders is negligible. The damage to foundation could not be observed visually during the inspection. Figure 11.1 illustrates the possible options for the restoration and rehabilitation of the bridge. The first option is to jack up the superstructure and to translate to its original position as illustrated in Figure 11.1(a).

The second option is to widen the piers and to support the abutment with a RC liner. Furthermore, new shoes (bearings) must be installed at appropriate positions. Furthermore, damaged cross girders and damaged main girders must be repaired. The residual strength of the bridge must be computed in order to check its capacity before the restoration works start. In addition, it is highly recommended to execute regular inspections to prevent the failure of the bridges and consequent accidents. Nevertheless, a new bridge might be necessary if we consider that operation period of bridge and the extent of the damage by the earthquake.

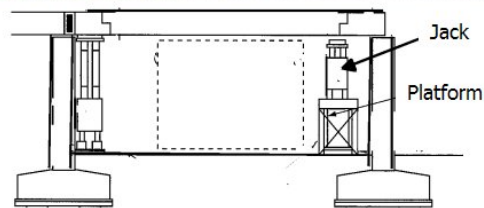
Balakot suspension bridge is a pedestrian suspension bridge. The bridge is severely damaged and upper parts of both abutments are displaced by about 20cm to SE direction. And superstructure is heavily deformed like an S-shape. It would be advisable to construct a new bridge in view of the damaged state of the bridge. Nevertheless, the abutments of the suspension bridge can be repaired as illustrated in Figure 11.2. Furthermore, it is highly recommended that precise measurements of the damaged bridges must be performed.



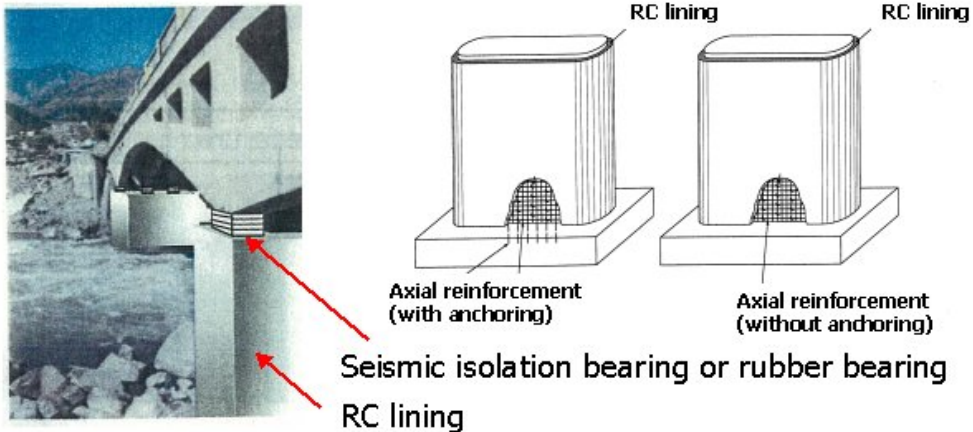
(1) Translation of girder by jacking



Example of work



(2) Widening of piers by addition of RC lining



(3) Repairing the damaged girder



Figure 11.1 Recommendations of possible options for restoration of Balakot bridge

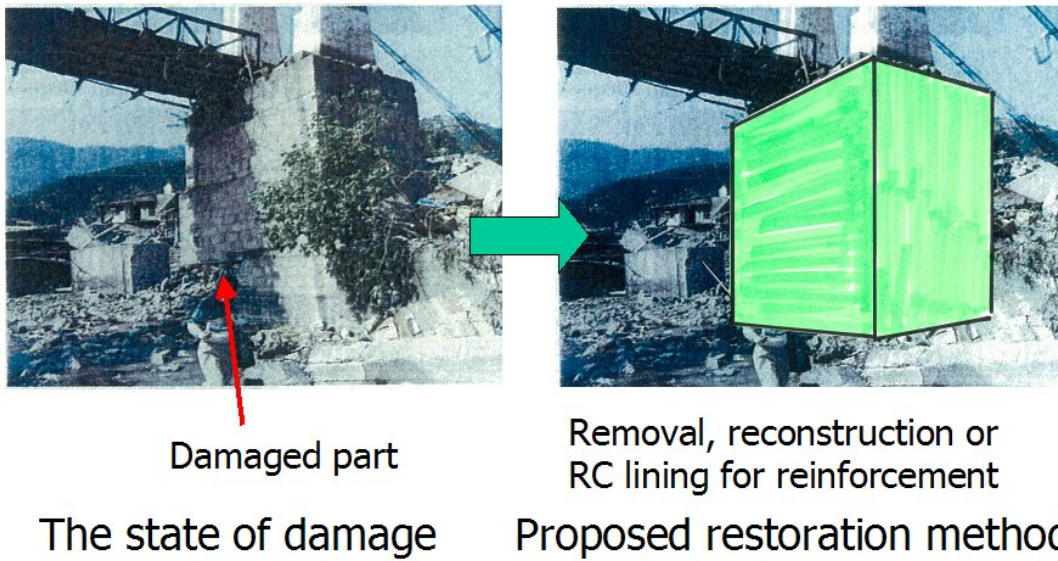


Figure 11.2 Recommendation for the restoration of Balakot pedestrian bridge

Next we describe our recommendations for the three damaged bridges along the roadway in Jhelum Valley between Muzaffarabad and Chakoti. The first damaged bridge is located 5 km south east of Muzaffarabad city. This bridge is a single girder bridge, which is under construction. Its north-west side of the girder was fell down to ground. The abutment was of stone masonry and it failed during the shaking of the earthquake. It is recommended to construct a new bridge along the present bridge as a permanent measure. However, if the existing girder is to be restored, then it is recommended to construct reinforced concrete abutments instead of stone masonry abutments.



Figure 11.3 New bridge recommendation for the damaged bridge with the use of existing girder

The top side part of arch masonry superstructure collapsed partially as a result of earthquake shaking. The collapsed section may be repaired by casting a new concrete liner. The east masonry abutment of the bridge damaged by the earthquake and it is recommended to cast a peripheral concrete and install ground anchors as illustrated in Figure 11.4.



Figure 11.4 Recommendation for the restoration of the damaged arch bridge

The west abutment of third bridge along the Jhelum Valley was partially damaged by the earthquake. As a temporary measure, an emergency bridge was installed. As for permanent measure, the box culvert is suitable for this bridge in view of its span (Figure 11.5).



Figure 11.5 Recommendation for the construction of a box-culvert for the damaged bridge

11.2 Recommendations for Roadway Embankments

The embankments of roadways failed along the rivers. Stone masonry or gabions are commonly used for supporting the embankments of roadways in steep terrain as well as along rivers. However, the embankments of roadways are not generally protected by retaining walls or gabions for a great length, which may make them prone to slopes as a result of toe erosion due to fast river currents. They may also suffer from heavy rainfalls in long-term. Therefore some measures should be undertaken either by reducing the slope of natural embankments or constructing gabions and retaining walls. Figure 11.6 illustrates a protection procedure for the collapsed section of the embankment.



Figure 11.6 A recommended protection procedure for the collapsed section of the embankment.

11.3 Recommendations for Slope Cuts

No support or protection measures for most of slope cuts along roadways is undertaken. Furthermore, the slope cuts are generally very steep and there are no catchment pockets in case of rockfalls and small scale slope failures. Figures 11.7 and 11.8 show examples of slope-cut in rock with fallen debris caused by the earthquake and recommended procedures how to rehabilitate the slope-cuts.

The most important issue is how to select the appropriate slope angle in relation to the geological features of slopes and slope height. For this purpose some empirical guidelines can be used as a preliminary assessment of the slope-cuts as they are outcomes of past records and case studies. Tables 11.1 and 11.2 gives the fundamental guidelines used in Japan for assessing the slope-cuts in soil and in rockmass. However, it must be noted that the geological features must be paid the utmost attention to particularly rock slopes as the empirical guidelines may sometimes be mis-leading.

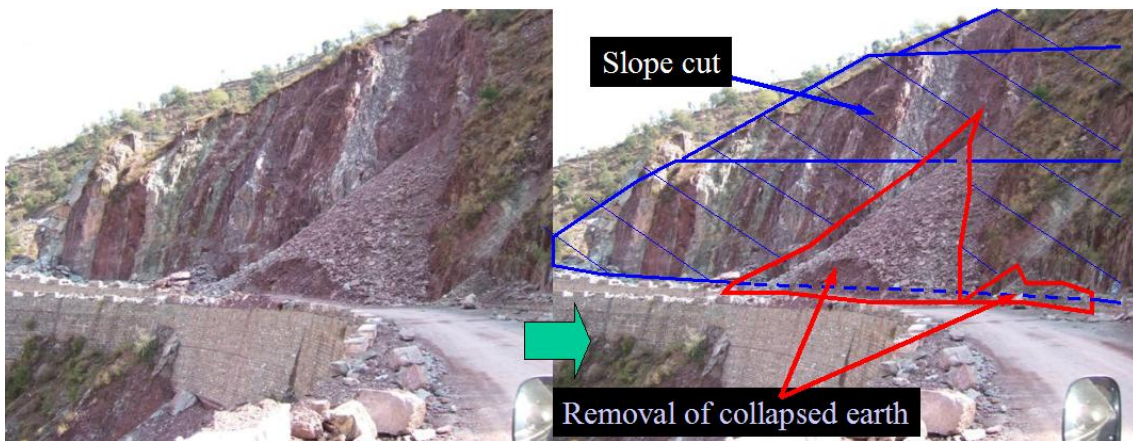


Figure 11.7 Recommendation for the restoration of slope-cut with fallen debris



(a) Against planar sliding

(b) Against flexural toppling failure

Figure 11.8 recommended slope-cuts in layered rock mass

Table 11.1 Empirical guidelines for slope-cuts in rock mass

ROCK OR SOIL TYPE		SLOPE HEIGHT	JH	JR	ROADWAY TECHNOLOGY STANDARD	KASEN-SABO TECHNOLOGY STANDARD	CODE FOR SAFETY OF WORKERS	STANDARD OF HOUSE SITE DEVELOPMENT OF YOKOHAMA
ROCK MASS	HARD ROCK		1 : 0.3~0.8 (0.5)	1 : 0.3~0.8 (0.5)	1 : 0.1~0.3 (0.2)		— 0 — 5 m 75° ↓ (Av.0.3)	
	FAIR ROCK		1 : 0.5~1.2 (0.8)	1 : 0.8~1.0 (0.9)	HARD 1 : 0.3 ~0.6 ↓ SOFT 1 : 0.5 ~1.0 (0.6)		— 0 — 5 m 80° 60°	
	SOFT ROCK			1 : 0.8~1.2 (1.0)	HARD 1 : 0.3 ~0.6 ↑ SOFT 1 : 0.8 ~1.2 (0.7)		— 0 — 5 m 50° 40°	

Table 11.2 Empirical guidelines for slope-cuts in soil

SOIL TYPE		SLOPE HEIGHT	JH	JR	ROADWAY TECHNOLOGY STANDARD	KASEN-SABO TECHNOLOGY STANDARD	CODE FOR SAFETY OF WORKERS	STANDARD OF HOUSE SITE DEVELOPMENT OF YOKOHAMA
STIFF & STABLE SOIL	SOIL WITH GRAVEL	0	1:0.8~1.0 1.0~1.2 (1.0)	1:1.0	1:1.0	1:1.0	0 2 5 m ↓ (Av.0.5)	0 5 m 45° 30°
		5						
		10						
STIFF & STABLE SOIL	SANDY SOIL	0	1:0.8~1.0 1.0~1.2 (1.0)	1:1.5 (1:1.3)	1:1.5 (1.1)	1:1.0 (1.0)	0 2 5 m ↓ (Av.0.5)	0 5 m 45° 30°
		5						
		10						
STIFF & STABLE SOIL	CLAYEY SOIL	0	1:0.8~1.0 1.0~1.2 (1.0)	1:1.5 (1:1.3)	1:1.5 (1.1)	1:1.0 (1.0)	0 2 5 m ↓ (Av.0.5)	0 5 m 45° 30°
		5						
		10						
LOOSE & UNSTABLE SOIL	SOIL WITH GRAVEL	0	1:1.0~1.2 1.2~1.5 (1.2)	1:1.5 ~1.8 (1.6)	1:1.5 (1.5)	1:1.5 (1.5)	0 5 m 45° 30°	
		5						
	SANDY SOIL	0	1:1.0~1.2 1.2~1.5 (1.2)	1:1.5 ~1.8 (1.6)	1:1.5 (1.5)	1:1.5 (1.5)	0 5 m 45° 30°	
		5						
CLAYEY SOIL	0	1:1.0~1.2 1.2~1.5 (1.6)	1:1.5 ~1.0 (1.6)	1:1.5 (1.5)	1:1.5 (1.5)	0 5 m 45° 30°		
	5							
CLAYEY SOIL WITH ROCK BLOCKS	0	1:1.0~1.2 1.2~1.5 (1.2)	1:1.5 ~1.0 (1.6)	1:1.5 (1.5)	1:1.5 (1.5)	0 5 m 45° 30°		
	5							

11.4 Recommendations for Alternative Roadway Routes

The epicentral area is a mountainous terrain and it is highly susceptible to slope failures and rockfalls, which may be very catastrophic sometimes. Furthermore, the slopes are very steep and covered with fallen debris. With due considerations of topography and possibility of slope failures, several alternative routes would be desirable for the area in case of blockage of roadways by rockfalls or slope failures. Figures 11.9 & 11.10 show examples of alternative bridge, viaducts or tunnels in mountainous terrain in Balakot area. Figure 11.11 show an alternative recommendation for the route nearby Muzaffarabad city.



Figure 11.9 An example of alternative bridge re-routing for Balakot area.



Figure 11.10 An example of combined viaduct-tunnel re-routing for Balakot area

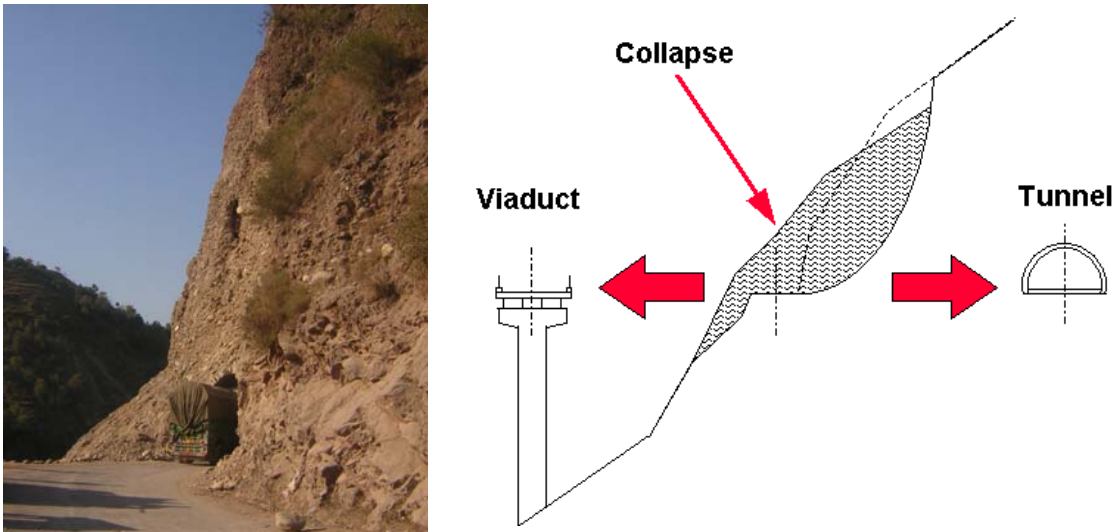


Figure 11.11 Recommendation of viaduct or tunnel construction for the route nearby Muzaffarabad city

11.5 Recommendations for Slope Stability Assessments

Kashmir region is very mountainous terrain and it is very much prone to slope failures in short and long term due to seismic shaking and/or rainfalls. Slope stability assessments should be carried out for the hazard mapping of the epicentral area. The slope stability assessments can be fundamentally carried out in two stages:

- 1) Macro-scale Stability assessment
 - a) Image Analysis
 - Aerial Photographs
 - Satellite Images
 - b) GIS-Based Stability Assessment
 - Topography(inclination, height etc.)
 - Rainfall
 - Vegetation
 - Past Records of Failures
- 2) Site-specific Stability Assessments
 - a) Empirical Methods
 - b) Kinematic Methods
 - c) Analytical Methods

11.5.1 Macro-scale Stability Assessment

The fundamental purpose of the macroscopic stability assessment is to identify the locations prone or experienced stability problems. For this purpose, the utilization of satellite images and aerial photographs is a very powerful technique to identify the areal extent of stability problems. Figure 11.12 shows an example of utilization of satellite images processed by Japan Geographical Survey Institute (JGSI) for identifying the locations of slope failures caused by this earthquake. It should be noted that this type assessment must be followed by site investigations and explorations.

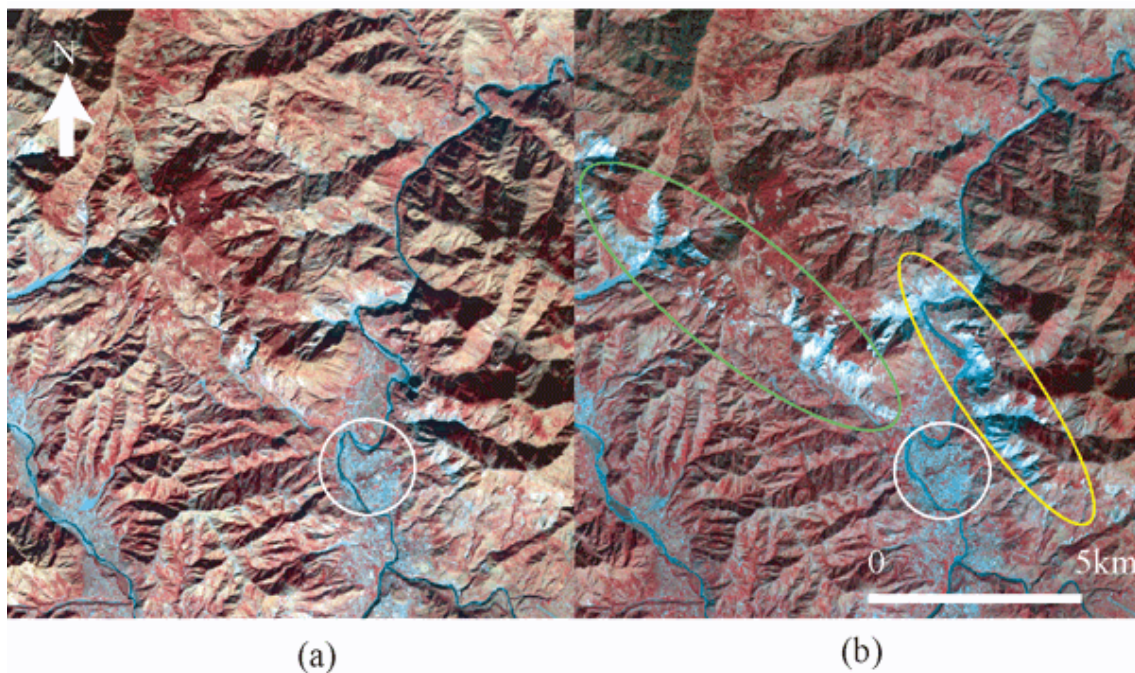


Figure 11.12 Utilization of satellite images for slope stability problems (JGSI, 2005)

It is also known that the regional and local tectonic features (faults, folding etc.) have great influences on the characteristics of geo-material constituting slopes and the possible mode of slope failure. It is known that when the regions experienced or experiencing tectonic movements, rockmass would be disturbed and there will be numerous structural features, which may cause severe slope stability problems together with loadings resulting from gravity, rainfall and/or seismic shaking. The recent earthquakes in Japan and other countries indicated that very large slope failures caused by earthquakes entirely depend upon the structural geological features (i.e. faults, folds, bedding planes) of regions. Figure 11.13 shows slope failures in Shizuoka prefecture of Japan where four major plates, namely, Euroasia, Pacific, Philippine Sea and North America plates confluence with each other.

weightings of rainfall, seismicity, geological features and past records of slope failures, some analytical stability assessments are recently being incorporated within the GIS systems. Nevertheless, the level of analytical stability assessment methods incorporated in the GIS systems for slope failure hazard mapping is far behind the actual level of slope engineering.

11.5.2 Site-specific Slope Stability Assessment

Site-specific slope stability assessment is fundamentally classified into three categories:

- Empirical Methods
- Kinematic Methods
- Analytical Methods

There are many empirical methods, which are outcomes of rich past experiences on slope stabilities. Tables 11.1 and 11.2 prepared by major governmental and local authorities. Particularly, Japan Highway Authority (JH) and Japan Railways (JR) provide basic guidelines how to design (slope angle) and how to assess the stability of slopes depending upon the ground conditions (rock or soil) and slope height without any particular emphasis on neither rainfalls or earthquakes. For example, the JH empirical criteria suggest the recommended slope angles for ground containing gravels (or cobbles) should be less than 40-51°. For the similar ground conditions, JR recommends that slope angle must be less than 45°. When we apply these empirical criteria to failed slopes of ground containing large cobbles in both Balakot and Muzaffarabad, it is understood that the initial slope angle of the failed slopes were greater than 60° (Figure 11.15).



Figure 11.15 Some examples of slope failures in ground containing cobbles

Kinematic analyses are generally for the stability assessments of rock slopes on the bases of prominent discontinuities such as faults, throughgoing discontinuities (bedding plane, foliation, sheeting joints ect.) and their frictional properties. Figure 11.16 shows a guideline how to kinematically assess the possible rock slope failures. Figure 11.17 shows an application of the kinematic assessment method with the consideration of seismic coefficient for the Tsaoling rock slope failure caused by 1999 Chi-chi (Taiwan) earthquake.

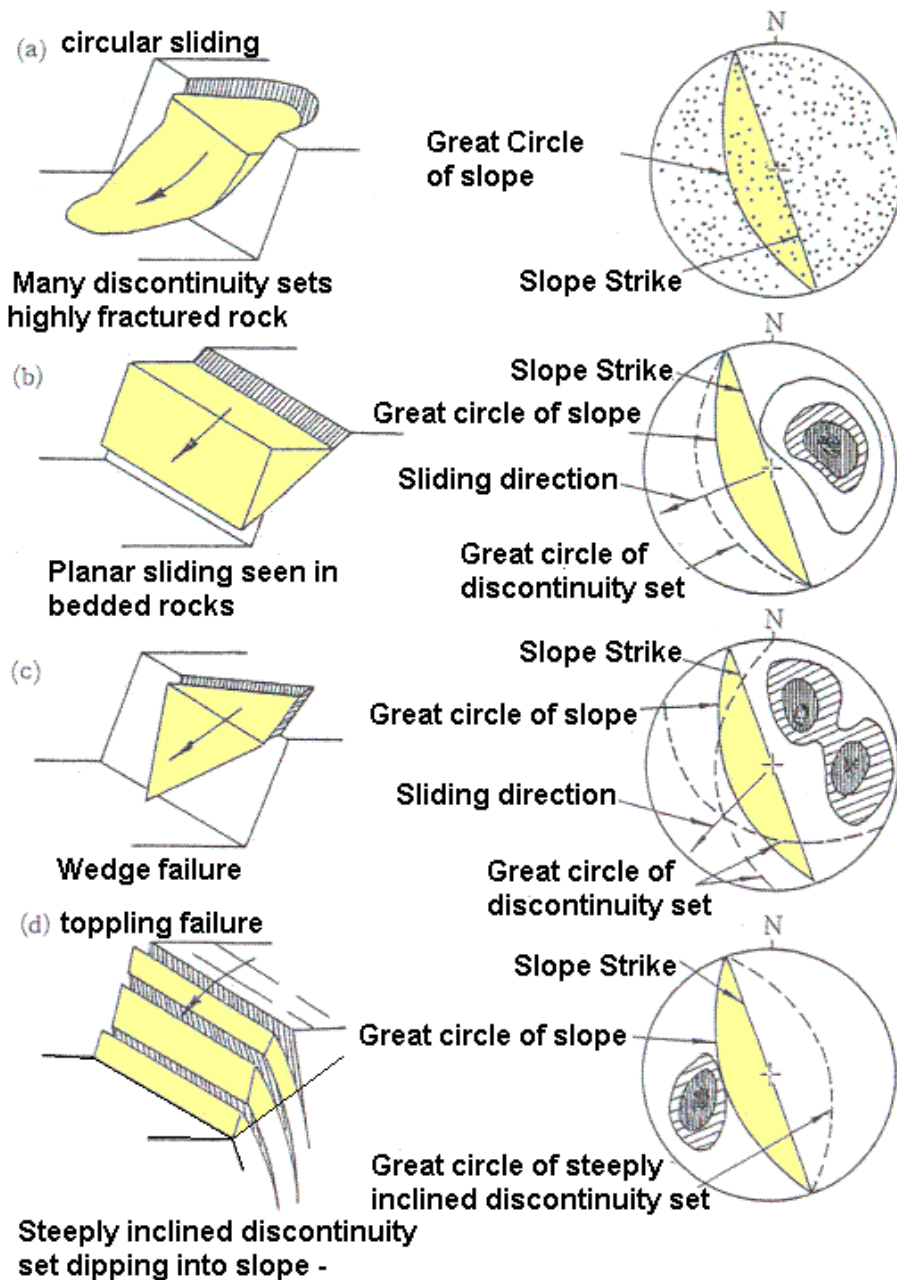


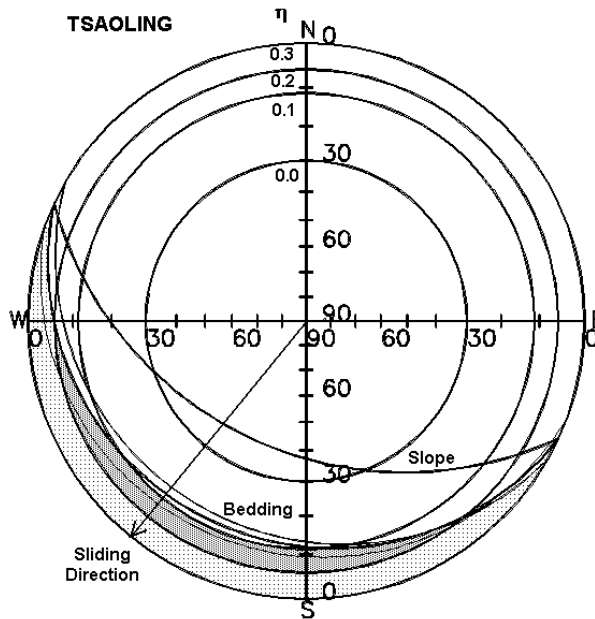
Figure 11.16 Kinematic stability assessment of rock slopes (from Hoek & Bray, 1977)



(a) Satellite image



(b) Land view



(c) Kinematic analysis of slope sliding

Figure 11.17 A kinematic analysis of Tsaoiling landslide (from Aydan, 2000)

Furthermore, several kinematic stability analyses methods for blocky rock mass are proposed with the consideration of seismic loading ($\eta = a_H / g$) and the inclination of throughgoing discontinuity set (such as bedding plane, schistosity or foliation etc.) and intermittency angle (ξ) (Shimizu et al. 1987, Aydan 2000). Figure 11.18 shows stability assessment charts under seismic loading for blocky rock masses. This type kinematic analysis should provide the most likely locations of slope failures for a rapid stability assessment for a large area with the consideration of discontinuities and seismic coefficient. However, it should be noted that the kinematic analyses assume that the slope failure are only associated with the sliding and/or separation of discontinuity sets, and it requires frictional characteristics and orientations of discontinuities as primary parameters.

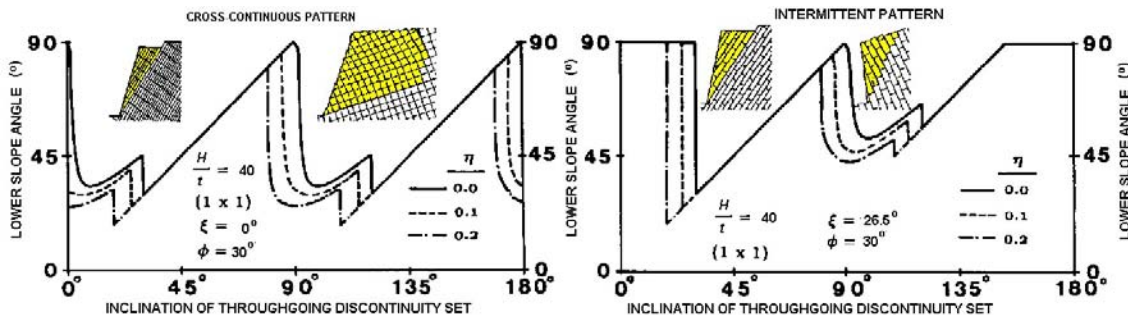


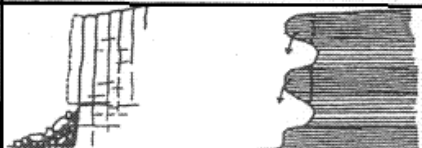
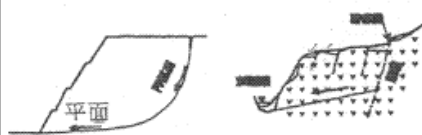
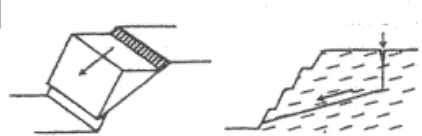
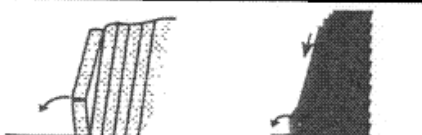
Figure 11.18 Stability assessment charts under seismic loading for blocky rock masses

Analytical Stability Assessment involves the analysis of a particular site using various methods of stability analysis. Such analyses require information on both the geometry of the slope, loading conditions (gravity, seismic, traffic, blasting), ground water conditions and properties of soil, rock, discontinuities and their orientation parameters. Since geotechnical investigations is covered in the next sub-section, the emphasis is given to the analytical stability assessment herein. Analytical stability assessment methods involves mainly limiting equilibrium methods and numerical methods. Figure 11.19 illustrates the analytical methods used in slope engineering for various modes of failure. Compared to the limiting equilibrium methods, the utilization of numerical methods is not so wide-spread. Nevertheless, many numerical methods such as FEM, FEM with joint or interface element, DEM, DDA, RBSM, DFEM etc. are developed and used in the assessment of soil and rock slopes with advance in computer technology. This type of analyses would be required when the geology and/or the mechanical behaviour of materials of the slope and loading conditions are very complex.

The most simple methods are based on the limiting equilibrium concept. If such methods are utilized, then the mode of failure must be assigned and the geometry of surface of failure must be either designated or obtained through an iterative minimization technique. The available limiting equilibrium methods for various failure modes of slopes are:

- a) Curved surface sliding (Bishop, 1955; Janbu, 1968)
- b) Planar sliding (Coulomb, 1776; Terzaghi, 1950)
- c) Planar sliding with tension crack (Hoek & Bray, 1977)
- d) Wedge sliding (Wittke, 1964; Hoek & Bray, 1977; Kovari & Fritz, 1975)
- e) Combined sliding and shearing (Aydan et al., 2001)
- f) Flexural toppling (Aydan & Kawamoto, 1987, 1989)
- g) Blocky toppling failure (Goodman & Bray, 1976; Aydan et al. 1989)
- h) Combined toppling and sliding failure (Aydan et al. 1989)

Depending upon the slope geometry and ground conditions, one or several failure modes are considered and safety factors are computed for assessing the slope stability. The system developed by Aydan et al. (1991) may be used for this purpose. Figure 11.20 illustrates the criteria for choosing likely failure modes for blocky rock mass.

FAILURE MODE		ILLUSTRATION	ANALYSIS METHOD			
			FEM,DFEM	DEM	DDA	LEM
ROCKFALL	SMALL SCALE		×	○	⊙	△
	LARGE SCALE		×	○	⊙	△
COMBINED SLIDING			⊙	○	△	○
PLANAR SLIDING			○	○	○	○
WEDGE FAILURE			○	⊙	△	○
FLEXURAL TOPPLING			△	○	⊙	○
BLOCK TOPPLING			△	⊙	⊙	○
BUCKLING			△	⊙	⊙	○

⊙ Often used ○ Commonly used △ Seldom used × Not used

Figure 11.19 A classification of analytical methods used for various failure modes

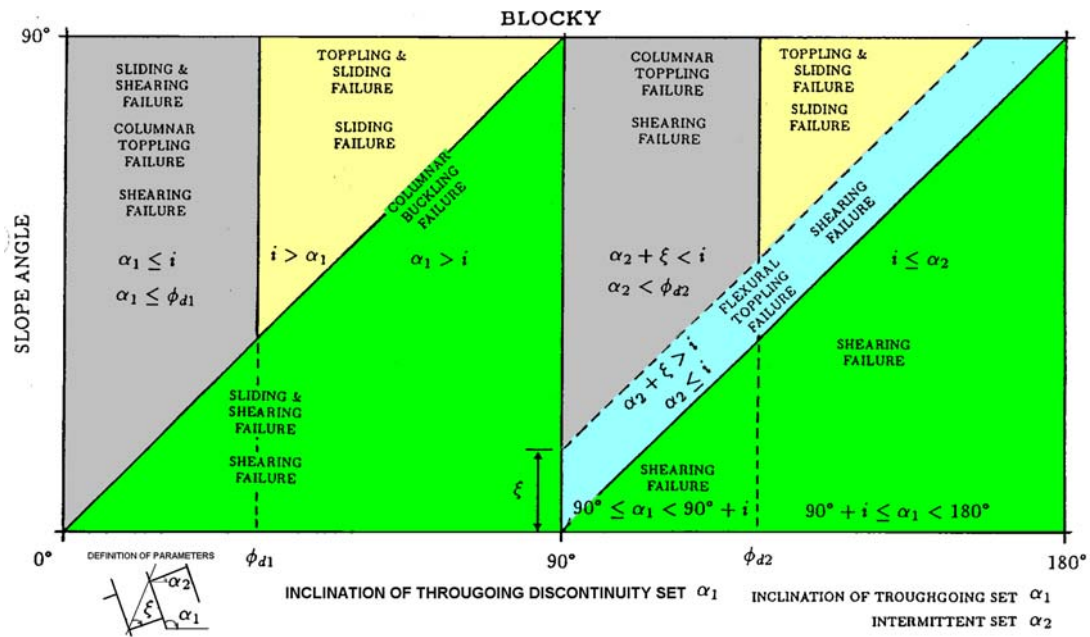


Figure 11.20 Illustration of the criteria for choosing failure modes for blocky rock mass

An example of stability analyses for failed slopes with cobbles observed in Balakot and Muzaffarabad is carried out using the planar sliding method. In the computations, the failure surface is obtained through the minimization procedure and computational results are plotted as a function of slope height and lower slope angle as shown in Figure 11.21. In the computation, the friction angle is taken as 40° since the measured repose angle at sites can be safely assumed to be equivalent to friction angle of failed soil. The normalized cohesion by soil unit weight was varied between 1 and 6 and the relation between slope height and slope angle for safety factor of 1 for a lateral seismic coefficient of 0.9, which is likely the ground acceleration levels at Balakot as well as Muzaffarabad, is computed. The normalized cohesion of soil with cobbles was inferred from needle penetration index tests to be ranging between 3 to 5. For these parameters, the slope failures would be observed when the slope height was greater than 7.7m. This computational result implies that some restrictions on either slope angle or slope height in the re-development of settlements in sloping ground must be implemented. It is also recommended that geotechnical parameters of ground should be measured before the commencement of re-construction.

Many soil or surficial slope failures seems to be influenced by the inclination of the bedding plane of rock units. If the stability analyses to be performed for such slopes it is highly recommended that one of the failure surface should be parallel to the bedding planes and the rest of the failure surface from the toe of the slope to the bedding plane

can be considered to be curved. Furthermore, the loads due to gravity, rainfalls and seismic forces should be considered in stability analyses since the epicentral area may further experience similar type earthquakes in the future.

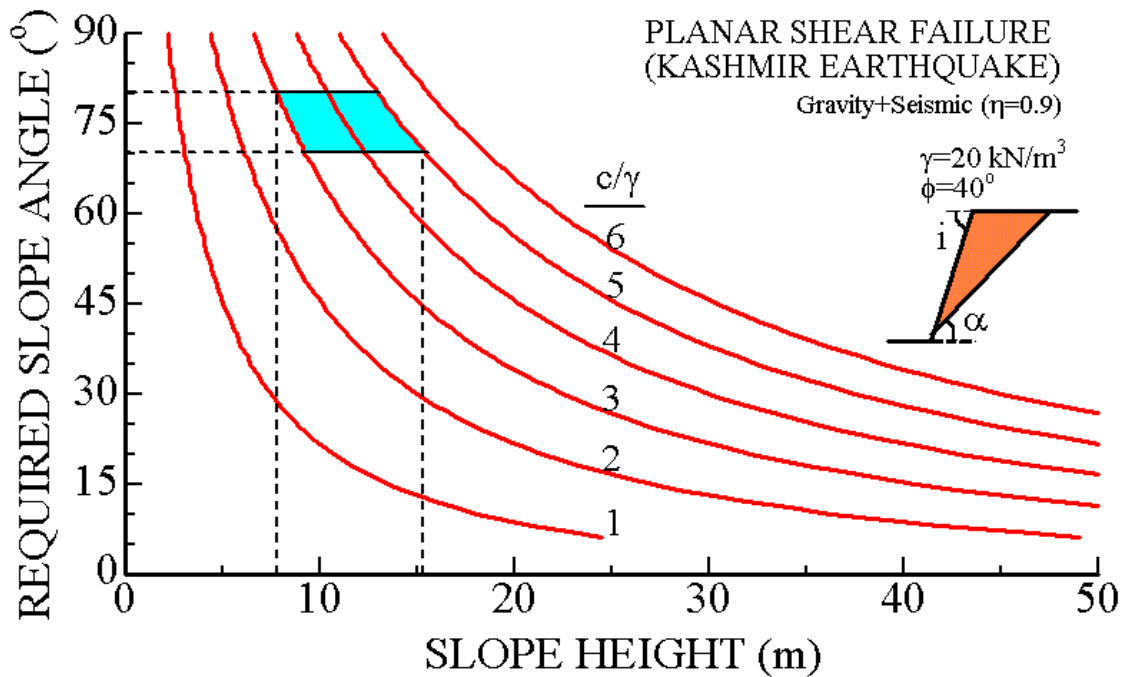


Figure 11.21 Computed slope angle and slope height relations for ground with cobbles

The geometrical configuration of mountains in the epicentral area is strongly influenced by geological folding process. The folding axis of the mountains generally ranges between N-S or NW-SE. The valleys are faulted and they may also correspond to either anticlines or synclines. As a result of these tectonic features, the mountain slopes are entirely governed by the throughgoing discontinuity set, namely, bedding plane. The measurements on the planes at several locations (nearby Balakot and along the route between Murree and Muzaffarabad) indicated that it ranges between 34 and 65°. The in-situ tilting tests revealed that the friction angle of bedding planes ranges between 30-40°, depending upon their surface morphology. The natural slope of mountains in the epicentral area ranges between 30 and 50°. When the bedding planes dip towards valley side, the natural slope angle of lower part of the mountain is almost equivalent to the inclination of bedding plane. This simply implies that the cohesion along the bedding planes is quite negligible. For the given height and tectonic features of rock mass, the natural analogy implies that the slopes would be resistant to pure shear failure or combined shear and sliding failure. However, when slopes are undercut as seen in Figure 11.22(a), the planar sliding failure of bedded rock mass would be caused.

Therefore, if the widening of present highways are to be carried out, the angle of slope cuts either should be either parallel to the bedding plane or reinforcement by rockbolts or rockanchors will be required.

The mountains with bedding planes dipping into mountain side are more stable and the slope angle is generally greater than 40°. It seems that the natural slope angle (i) of high mountains in relation to the bedding plane inclination (α) can be taken according to the following formula

$$i = \alpha - 90 + \beta$$

Where β is the rupture angle with respect to the normal of bedding plane. Its value generally ranges between 10-15° in view of both model tests and case studies (Goodman & Bray, 1976; Aydan & Kawamoto, 1989). The value of β for the natural slope angle of mountains of the epicentral area ranges between 10 and 12°. This implies that if the angle of slope cuts for roadways is in accordance with the above formula, there is no need for any reinforcement measure in bedded rock mass. Figure 11.23 shows an example of computations of slope angle and slope height relations for bedding plane inclination of 135°. Tensile strength of layers was inferred to be about 475 kPa in view of rock mass conditions in the epicentral area and in-situ tests on shale in a hydraulic power plant project in Akaishi region of Shizuoka prefecture, Japan. While the lower angle of rock slope can be very steep (90°) for a slope height of 6-10m (Figure 11.22(b)), the slope angle must be reduced in relation to the slope height when no reinforcement measure is implemented.



(a) Sliding slope failure due to undercutting (b) Stable slope against flexural toppling

Figure 11.22 Some examples for appropriate slope cutting in layered rock mass

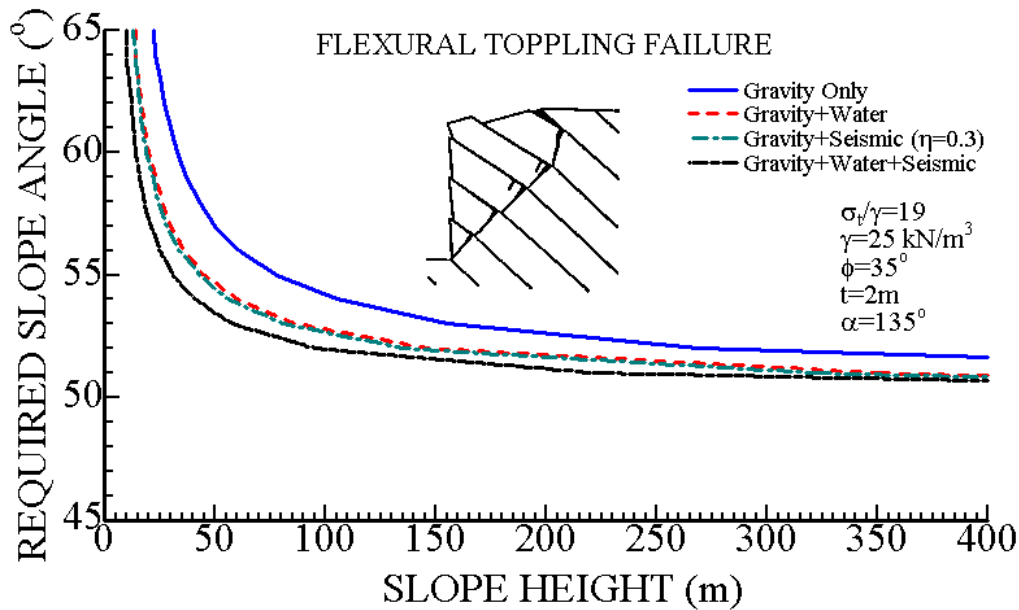


Figure 11.23 Computed slope angle and slope height relations for flexural toppling mode

11.6 Recommendations for Slope Stabilization

When the slope angle and/or slope height are greater than those required for natural stability, the slope stabilization measures would be necessary. Furthermore, slopes of soil and soft-sedimentary rocks may deteriorate or erode due to exposure to atmosphere, which may require the surface protection of slope surface. The possible measures for slope stabilization and slope protection may be listed as follows (Figure 11.24)

- a) Retaining Walls with or without fence (quite common)
- b) Gabions (common in protection against river erosion)
- c) Terre-armee (expensive to use)
- d) Rockbolting and Anchoring
- e) Drainage (should be gravitational, otherwise expensive)
- f) Wire-mesh or rockbolted frame (effective against rock-falls)
- h) Shotcreting (effective against gullying or deterioration)
- g) Rock Shade (effective against small scale rockfalls)
- i) Piling (effective but expensive)
- j) Berms and soil removal
- k) Tunnelling
- m) Viaduct construction
- n) Slope angle reduction (bench excavation)

Probably the item n) would be the most desirable measure, and the fundamental

concept should be such that the overall stability of the slope must be attained by the self-resistance of ground. Therefore, the stabilization measures should be kept to the minimum. When there are some occasions, that is, it is impossible to reduce slope angle due to slope-cut height, tunneling, viaduct construction may be an effective way of dealing with the problem (Figure 11.10). Figure 11.25 compares the cost of several measures for slope stabilization and protection in Japan.

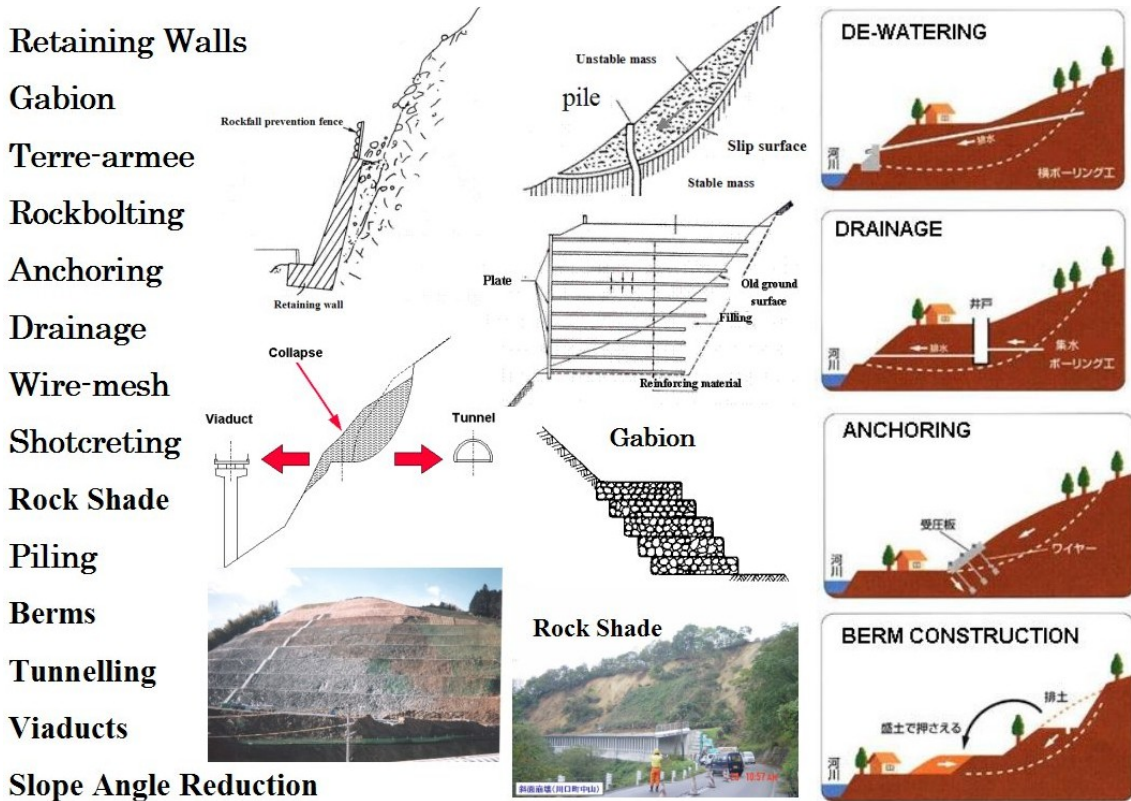


Figure 11. 24 An illustration of slope stabilization & protection measures

■ Approximate Cost

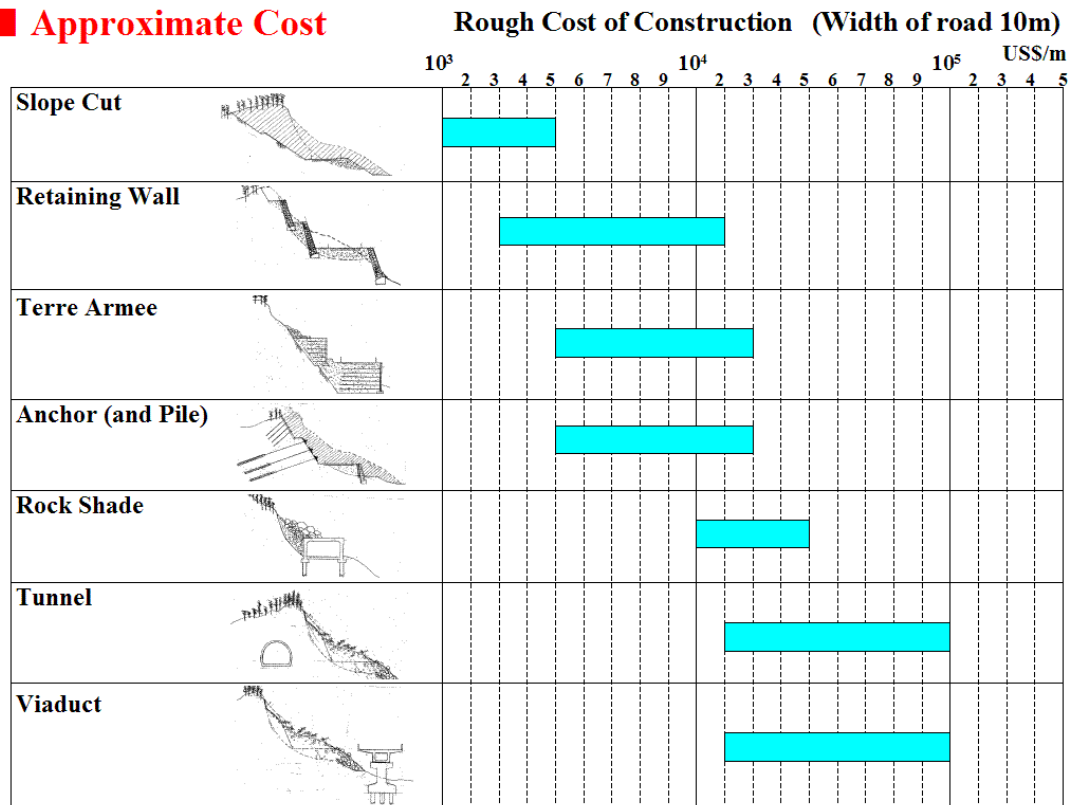


Figure 11.25 Comparison of the cost of several measures of slope stabilizations and protection in japan

11.7 Recommendations for Geotechnical Investigations for Damaged Civil Infra Structures & Slopes

Understanding the causes of damages to civil engineering structures such as bridges, roadways, embankments and natural slopes or slope cuts by earthquakes as well as their earthquake resistant design requires appropriate geotechnical investigations. The bearing capacity and lateral resistance of foundations of piers of bridges and the stability of abutments under the gravitational and earthquake loads require geotechnical characteristics of ground and embankment materials. Depending upon the ground conditions, various geotechnical investigations may be used. The geotechnical investigations may both involve laboratory tests and in-situ tests and/or in-situ explorations. Geotechnical investigations may be carried out mainly in two stages:

- a) Rapid geotechnical investigations
- b) Detailed geotechnical investigations.

The above investigations are described in the following sub-sections.

11.7.1 Rapid Geotechnical Investigations

Rapid geotechnical investigations and assessments are based on satellite or aerial photography of the area of interest and outcrop surveys. Satellite or aerial photographs would be quite useful to know the extent of damage to civil infra structures and to identify most critical locations for drawing emergency restoration and recovery plans. Figure 11.26 shows a rapid assessment of slope failures and their extent nearby Muzaffarabad city.

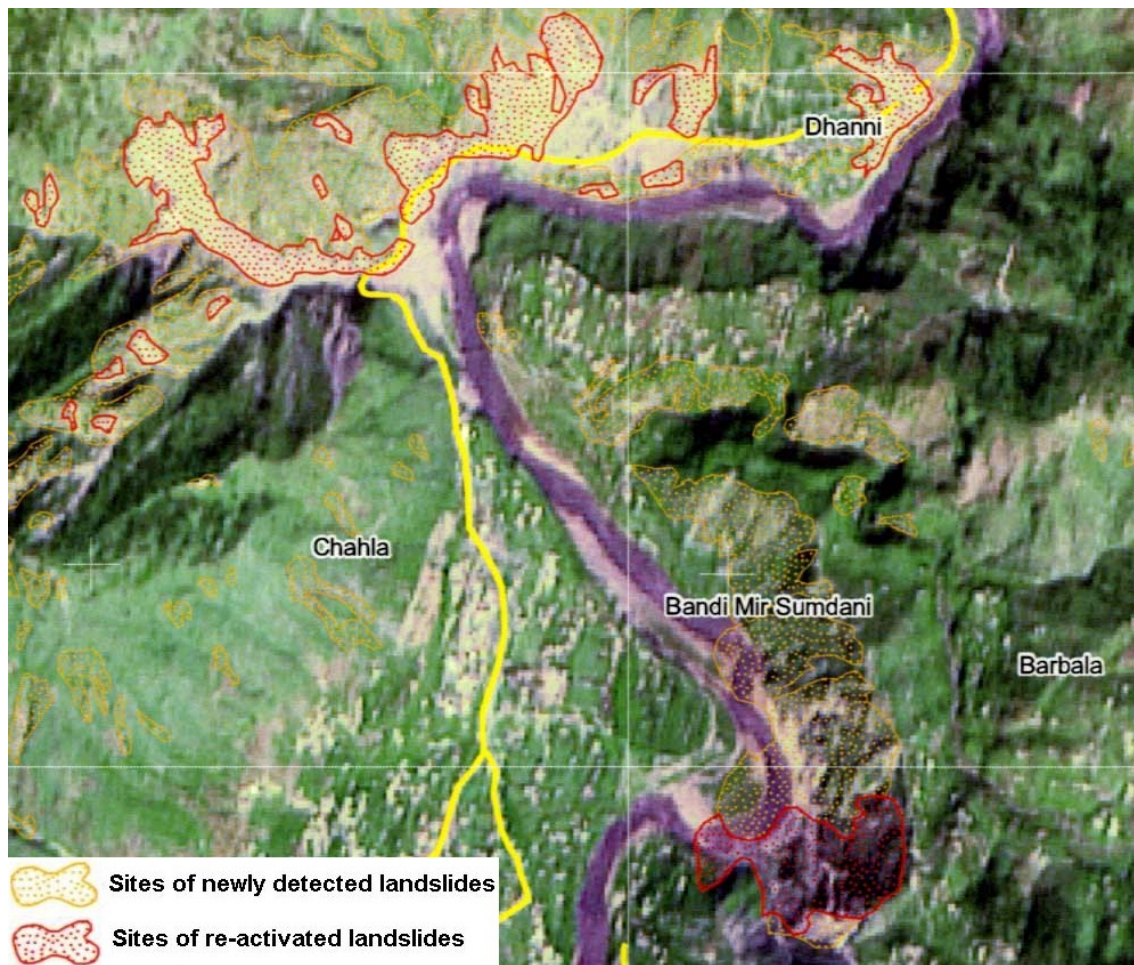


Figure 11.26 Rapid assessment of slope failures and their extent nearby Muzaffarabad city from satellite images

The next step is to carry out outcrop surveys to document the distribution of damaged area, existence of springs, geological features such as rock and soil units, the orientations, spacing and spatial distributions of discontinuities such as joints, faults, bedding planes etc. Furthermore, the possible location of failure surface or the causes of

damage to structures should be inferred, which may be quite important in planning the detailed investigations and required laboratory and in-situ tests. Figure 11.27 shows an example of outcrop survey of a landslide area in Chuetsu region of Niigata prefecture.



Figure 11.27 An example of outcrop survey of a landslide area

11.7.2 Detailed Geotechnical Investigations

Detailed geotechnical investigations mainly involves the following four items:

- a) Boring
- b) Sounding and Index Tests
- c) Tests (in-situ or laboratory)
- d) Observation and Monitoring

Boring is probably the best and direct method to investigate the geological and geotechnical conditions beneath piers, abutments, embankments and slopes. The number and length of boreholes are determined by considering the size of the structure. For example, at least three boreholes are drilled in a landslide area (Figure 11.28). As for bridge foundations the number of boreholes may be one or more. In order to assess the properties of rock mass, rock mass classifications should be carried out.

Sounding and index tests are often used to infer the in-situ properties of ground (soil or rock mass) with the use of past empirical relations. Sounding tests may involve standard penetration tests (SPT Tests), cone penetration tests, Swedish sounding test for soil-like ground, electrical resistivity (water table etc.), P-wave, S-wave and Rayleigh-wave investigations for soil and rockmass. Particularly the utilization of standard penetration test for soil-like ground is quite common in Japan since many empirical relations are developed for determining design parameters of structures. Seismic velocity index tests are generally used for bridge and pylon foundations. Figure 11.29 shows some examples of sounding tests.

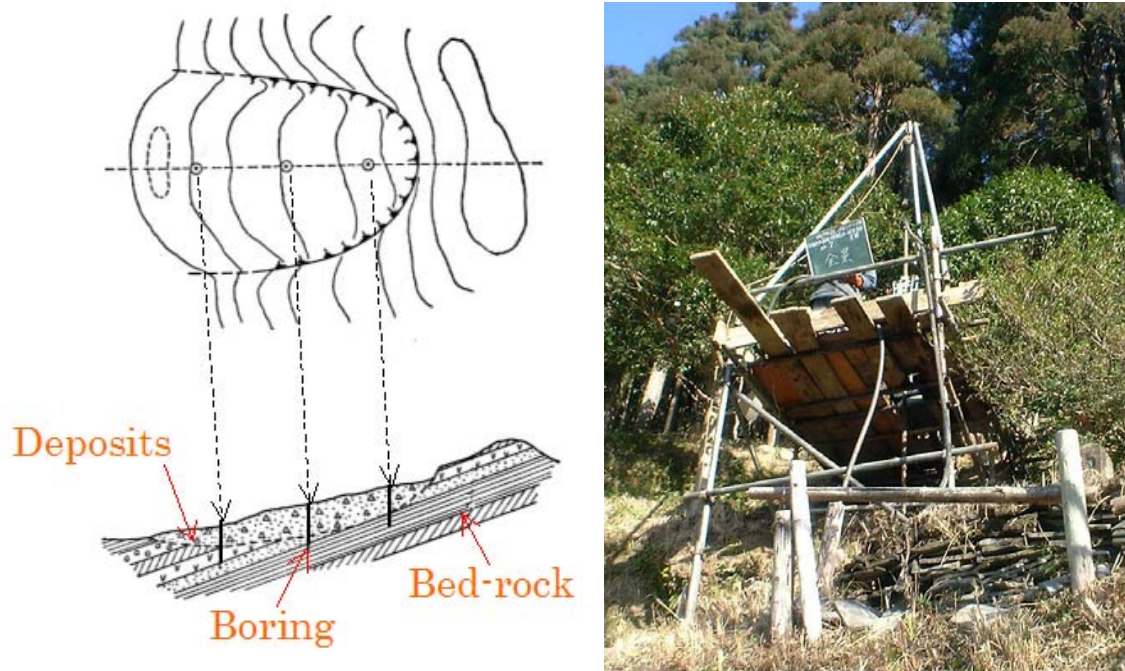


Figure 11.28 The layout of boreholes for landslide and an example of boring



(a) Standard penetration index test set-up



(b) seismic velocity sounding set-up



(c) Electrical resistivity sounding set-up

Figure 11.29 Some examples views of several sounding tests.

Tests on ground (soil or rock) are carried out in-situ and/or laboratory. The tests involve the determination of mechanical properties (i.e. deformability, strength properties etc.) of ground. One of the in-situ tests is called as elastometer test or pressuremeter test

(Figure 11.30). This test is commonly used in soil and soft ground. The test may also yield information on the strength properties of ground if their pressure level is high enough to yield the surrounding ground.

Shear strength tests on bridge foundations and rock discontinuities may also be required. Although shear tests on bridge foundation would be rare, the shear strength tests are necessary for assessing the stability of rock mass. The most simple test would be tilting test, which would generally yield the equivalent frictional properties of discontinuities. However, if the normal stress dependency of discontinuities is required then laboratory shear tests could be carried out on undisturbed samples of rock discontinuities. Furthermore, laboratory tests can be carried out on samples of ground. While the properties of soil-like ground can be directly utilized as in-situ properties, the laboratory tests on rock samples must not be used as the representative values of rock mass. This would require some further processing of properties determined from laboratory tests as well as rock mass evaluations using some rock classification techniques.



Figure 11.30 A view of elastometer (pressuremeter) test

11.8 Debris Management

The disposal of debris resulting from collapsed buildings and structures presents an extremely difficult problem in terms of environmental concerns in long term. On the other hand, the implementation of basic emergency measures requires quick disposal of debris. Therefore, it is essential to designate the areas of disposal of debris in case of emergency. Debris is sorted according to types of material and are disposed in designated areas in Japan (Figure 11.31(a)). Figure 11.31(b) shows an example of sieve plant that separates debris into several material groups. Only debris of concrete is used as aggregate for pavement construction. Ground or water pollution by disposed debris must be avoided.

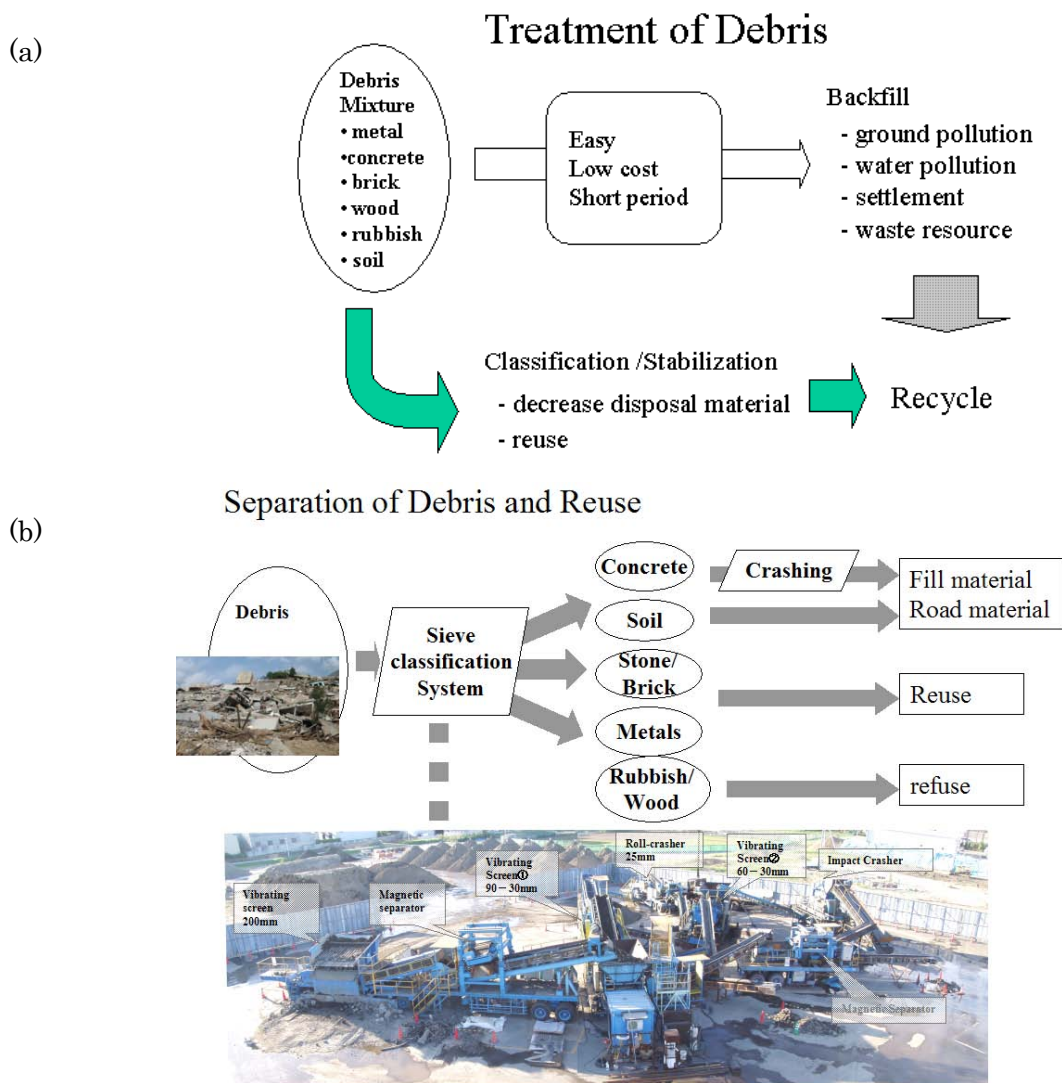


Figure 11.31 Treatment and separation-disposal of debris

12 CONCLUSIONS

In this report, an overall view of geology, tectonics, seismicity of 2005 Kashmir earthquake were presented and structural and geotechnical damages concerning civil engineering structures and buildings their possible causes were described. The maximum ground acceleration at Balakot was inferred to be at least 0.9-1.0G. The computational results indicated that the failure of soil slopes containing large cobbles was imminent under such ground strong motions. Furthermore, the loose surficial and talus deposits were laterally spreaded, which resulted in further damage in Balakot as well as in Muzaffarabad. In spite of the translation of the girder of Balakot bridge more than 1m, the bridge could stand against high ground motions and forces imposed by ground due to slope failures. Although some damage to several bridges were observed, it may be stated that large bridges with good engineering design and construction did stand against high ground motions.

Slope failures were observed along entire Neelum and Jhelum valleys. Particularly slope failures associated with heavily fractured dolomitic rock unit were spectacular in both scale and its areal distribution. However, these slope failures were aligned on locations which may be interpreted as the surface expression of the causative fault.

The recommendations of the support team for the temporary and permanent restoration and re-construction of the earthquake affected civil engineering structures are presented. The recommendations, which are described in detail in Chapter 11, can be briefly summarized as follows:

- 1) The horizontal forces must be taken into account during the design of bridge girders and they should be restrained through shear keys or anchors.
- 2) It is recommended to build bridges as redundant structures in areas with high ground shaking. In spite of horizontal damage of the bridge deck due to high ground shaking as well as permanent displacement of ground, the bridge of Balakot, which is designed as redundant structure, performed well.
- 3) The bridges of Balakot can be repaired using several techniques recommended in Chapter 11. However, it is highly recommended to properly evaluate the damages state of the bridge before its restoration and rehabilitation. Nevertheless, it will be advisable to built several new bridges.
- 4) The masonry abutments of bridges should be reinforced through anchors and reinforced concrete liners.

- 5) The both sides of the steep valleys should be connected to each other at certain intervals in order to facilitate by-pass routes in case of emergencies resulting from bridge collapses and/or slope failures.
- 6) Since the region is a mountainous terrane, it is recommended to built tunnels and/or viaducts when there is high risk of slope failures.
- 7) Embankment slopes are highly steep and they are prone to fail either by ground shaking or heavy rainfalls. It is recommended to either reduce slope angle of embankments or to introduce support, reinforcement or protection measurements. Furthermore, measures should be introduced to eliminate the toe erosion problems.
- 8) The slope angle and slope height of slope cuts should be such that the slope is stable under its natural resistance. If such a condition is difficult to be fulfilled, some measures for supporting and reinforcement should be undertaken. Since the valleys are very steep, there is high possibility of surficial slope failure risks.
- 9) The design of slopes and the assessment of failure risk must be based on the guidelines of modern slope engineering.
- 10) Natural slopes of the mountains are now in their equilibrium state. Unless some artificial disturbances are introduced, it is expected that the problems would be negligible.
- 11) Slopes of dolomitic rock unit along the fault line are susceptible further failures. Therefore, it is recommended that no permission for housing or structure construction should be given in such locations.
- 12) Housing and constructions on soil slopes containing large cobbles as observed in Balakot and Muzaffarabad should not be allowed. Although these slopes can be stable for high slope angles under static conditions, they are prone to failure during earthquakes. If the construction is allowed, there should be a safety zone between the slope crest and allowable construction boundary.

REFERENCES

- Aydan, Ö. and T. Kawamoto (1992). The stability of slopes and underground openings against flexural toppling and their stabilisation. *Rock Mechanics and Rock Engineering*, **25**(3), 143-165.
- Aydan, Ö. (2002): The inference of the earthquake fault and strong motions for Kutch earthquake of January 26, 2001. A symposium on the records and lessons from the recent large domestic and overseas earthquakes. Japan Earthquake Engineering Society, Tokyo, 135-140.
- Aydan, Ö., Y. Shimizu, Y. Ichikawa (1989). The Effective Failure Modes and Stability of Slopes in Rock Mass with Two Discontinuity Sets. *Rock Mechanics and Rock Engineering*, **22**(3), 163-188.
- Aydan, Ö., Y. Ichikawa, Y. Shimizu, and K. Murata (1991). An integrated system for the stability of rock slopes. *The 5th Int. Conf. on Computer Methods and Advances in Geomechanics*, Cairns, **1**, 469-465.
- Aydan, Ö., Shimizu, Y. & Kawamoto, T. 1992. The stability of rock slopes against combined shearing and sliding failures and their stabilization. Asian Regional Symposium on Rock Slopes, Oxford & IBH Pub. Co. Pvt. Ltd., New Delhi, pp 203-210.
- Aydan, Ö, H. Kumsar, R. Ulusay (2002): How to infer the possible mechanism and characteristics of earthquakes from the striations and ground surface traces of existing faults. JSCE, Earthquake and Structural Engineering Division, Vol.19, No.2, 199-208.
- Aydan, Ö., Seiki, T., Shimizu, Y. and Hamada, M. (2000): Some considerations on rock slope failures due to earthquakes. Chonqing-Waseda Joint Seminar on Chi-Chi Earthquake.
- Bilham, G. (2005): Kashmir earthquake 2005. <http://cires.colorado.edu/~bilham/Kashmir2005.htm>
- Bishop, A. W., 1955. The use of slip circle in the stability analysis of slopes. *Geotechnique*, v 5, pp 7-17.
- European-Mediterranean Seismological Center (EMSC) (2005): Earthquake Mw 7.6 in Pakistan October 8th, 2005. <http://www.emsc-csem.org/>
- Harvard (2004): Magnitude 7.6 PAKISTAN, Saturday, October 08, 2005 at 03:50:40 UTC. <http://www.seismology.harvard.edu/>
- Hoek, E. & Bray, J.W (1977): Rock slope engineering. Ed. Inst. Min. & Metall., Revised 2nd Ed., London.
- Geological Survey of Pakistan (2005): Tectonics, geology and seismicity of epicentral area. <http://www.gsp.gov.pk/>
- International GPS service (2005): Global time series. <http://www-gpsg.mit.edu/>

- Janbu N (1973) Slope stability computation. In: Embankment Dam Engineering, Cassagrande Volume, R.C. Hirschfield and S.J. Poulos (eds), John Wiley and Sons, N.York, pp 47-86.
- JGSI (2005): Northern Pakistan Earthquake, October 8, 2005 . <http://www.gsi.go.jp/>
- Okawa, I. (2005): Strong earthquake motion recordings during the Pakistan, 2005/10/8, Earthquake. <http://www.bri.go.jp/>
- Kovari, K., Fritz, P. (1975): Stability analysis of rock slopes for plane and wedge failure with the aid of a programmable pocket calculator. 16th US Rock Mech. Symp., Minneapolis, USA, 25-33.
- Martin Vallée (2005): Mw=7.7 05/10/08 Pakistan earthquake. Géosciences Azur, IRD, Nice, France, vallee@geoazur.unice.fr.
- Matsuda, T. (1981): Active faults and damaging earthquakes in japan. Macroseismic zoning and precaution fault zones. Maurice Ewing Ser., 4, Am. Geophys. Union, Washington, 271-289.
- Najman, Y., Pringle, M., Godin, L, and Oliver, G. (2002). A reinterpretation of the Balakot Formation: Implications for the tectonics of the NW Himalaya, Pakistan. TECTONICS, VOL. 21, NO. 5, 1045,
- USGS Global Seismographic Network (2005): Magnitude 7.6 - PAKISTAN 2005 October 8 03:50:40 UTC. <http://neic.usgs.gov/>
- UN (2005): South Asia – Earthquake Oct 2005. <http://www.reliefweb.int/>
- Wittke, W. (1964): A numerical method of calculating the stability of slopes in rocks with systems of plane joints. (in German) Felsmechanik und Ingenieur-geologie, Suppl. 1, 103-129.
- Yamanaka, Y. (ERI) (2005): EIC Seismological Note No. 171: Pakistan Earthquake (M7.6). http://www.eri.u-tokyo.ac.jp/sanchu/Seismo_Note/2005/EIC171ea.html
- Yagi, Y. (2004): Preliminary results of rupture process for Pakistan earthquake. <http://iisee.kenken.go.jp/staff/yagi/eq/Sumatra2004/Sumatra2004.html>